DEVELOPMENT OF COMPUTER MODELS FOR CORRELATING DATA OF FILM COOLING OF NOSE CONE UNDER HYPERSONIC FLOW

Semi-Annual Status Report
(April 1, 1986 to September 30, 1986)

Grant No. NAG-1-408

Principal Investigator: L. Sharpe, Jr.

North Carolina A&T State University
Greensboro, NC 27411

ABSTRACT

A 12.5 degree half cone with tangential slot injection at Mach 6.95 was studied to determine the heating rates to the surface of the body near and far downstream of the slot. The cone had a zero degree angle of attack. The heating rates were obtained using a computer program that was developed at NASA-Langley Research Center. The concentration of nitrogen from the slot into the boundary layer was also determined. The ratio of slot to freestream was varied to determine its effect on heating. The numerical heating rates were compared to other correlations obtained from experimental studies as well as theoretical laminar and turbulent results.

TABLE OF CONTENTS

LIST OF ILLUSTRATIONS

NOMENCLATURE

A	Surface area for heat transfer
C_p	Specific heat at constant pressure
C	Mass concentration of species
g	Ratio of local to edge concentration of species
h	Static enthalpy
U	Heat transfer coefficient (unit thermal conductance)
H	Total enthalpy, $h + u^2/2$
L	Reference length
ℓ	Mixing length
M	Mach number
m	Computation grid index in x-direction
n	Computational grid index in y-direction
p	Pressure
Pr	Prandtl number
q	Heat transfer rate
R	Local recovery factor
r	Dimensionless body radius, r_w/L
Sc	Schmidt number
t	Temperature
u	Mean physical velocity in streamwise direction
v	Mean physical velocity in direction Normal to surface
x	Streamwise direction in physical coordinate system
y	Direction normal to surface in physical coordinate system

GREEK SYMBOLS:

ε	Eddy viscosity for turbulent flow
θ	Circumferential angle
κ	Total eddy conductivity for turbulent flow
μ	Molecular viscosity
ρ	Density
τ	Stress

SUBSCRIPTS:

i	Species
w	at the wall
t	Turbulent
e	Free-stream
s	stagnation

CHAPTER I

INTRODUCTION

A solid body travelling at a high speed in air experiences a rise in its adiabatic wall temperature. This rise in surface temperature is largely caused by frictional heating. Re-entry vehicles, missiles, and hypersonic jet planes are all effected by frictional heating. The adiabatic wall temperature can rise as much as 57°F above that of free-stream air for flight speeds of 600 mph. A rocket travelling at 3600 mph can experience a rise in wall temperature of 1940°F [1]. This very high temperature can cause structural damage and can also cause property changes in the surface of the body.

One method developed to control the rise in surface temperature was slot injection film cooling. In this process, a fluid is injected through slots into the boundary layer on the surface to be protected.

The purpose of this study was to determine the heating rates on the surface of a cone shaped body. A computer program by Beckwith and Bushnell [2] was utilized to obtain the required heating rates numerically. The preliminary data used in the computer program was obtained from an experimental study of 12.5 degree half-angle cone with tangential slot injection of nitrogen into hypersonic flow. The experiment was conducted in an 8-foot temperature tunnel at NASA Langley Research Center in Hampton, Virginia [3].

The numerical results from this study were compared with heat transfer rates from a theoretical laminar study by Hamilton [4], a theoretical turbulent study by Johnson and Rubesin [1], correlations from an experimental study by Parthasarathy and Zakkay [5] and an experimental study by Zakkay et. al., [6]. The ratio of free-stream velocity to slot velocity was varied to determine its effects on the heating rates to the surface of the cone as well as the overall mixing process. The concentration of nitrogen in the boundary layer was also obtained.

CHAPTER II

PREVIOUS WORK

A solid body travelling at a high speed in air experiences a large increase in adiabatic surface temperature due to frictional heating. Johnson and Rubesin [1] examined analytical and experimental investigations appearing in the literature for heat transfer for submerged flow over flat plates, wedges, cones, cylinders and pipes. They presented evidence which supports the modified Newton's Law of Cooling equation as the fundamental heat transfer relation (See. Eq. 1).

$$\dot{q} = U A [t_w - (t_e + \frac{R u_e^2}{2C_p})] \tag{1}$$

where the term, $\frac{R u_e^2}{2C_p}$, accounts for the influence of frictional dissipation. A need to increase the number of investigations which determined heat transfer measurements with frictional heating was indicated by Johnson and Rubesin [1].

Beckwith [7] reviewed the studies that had been done to determine heat transfer measurements with frictional heating. He examined studies which indicates that incompressible flow, for two dimensional and zero-mass transfer application, had been extensively treated and a considerable number of methods could now predict the integral flow parameters. He indicated that the relations between the fluctuating flow correlations and mean flow quantities were indeterminate, thus theoretical predictions had to be evaluated by comparisons

with experimental data. He concluded that more detailed and reliable experimental data for both mean and fluctuating flow properties within turbulent boundary layers for a wide range of parameters were needed. He also noted that the finite difference method offered an advantage over some methods of solution in the sense that simple equations can be used to model the turbulent flux term.

With an increased understanding of turbulent boundary layers, investigations were conducted with the objective to protect a solid surface exposed to high temperatures. One method was to introduce a secondary fluid into the boundary layer on the surface to be protected. Goldstein [8] indicated that film cooling is one of the several means developed to introduce this secondary fluid. Film cooling is a technique where a secondary fluid is injected through slots and or holes in the surface. Three ways of introducing the secondary fluid are:

1. Slot injection
2. Jet injection
3. Transpiration

In slot injection film cooling, the fluid is injected through slots or holes directly into the boundary layer at one or more discrete locations. In jet injection film cooling, the secondary fluid is injected counter to the mainstream flow. Transpiration cooling is the process where the surface of a body is made of porous material and the secondary fluid enters the boundary layer through the permeable surface. The three ways of introducing the secondary fluid are shown in figure 1. The present study will be concerned only with film cooling by slot injection.

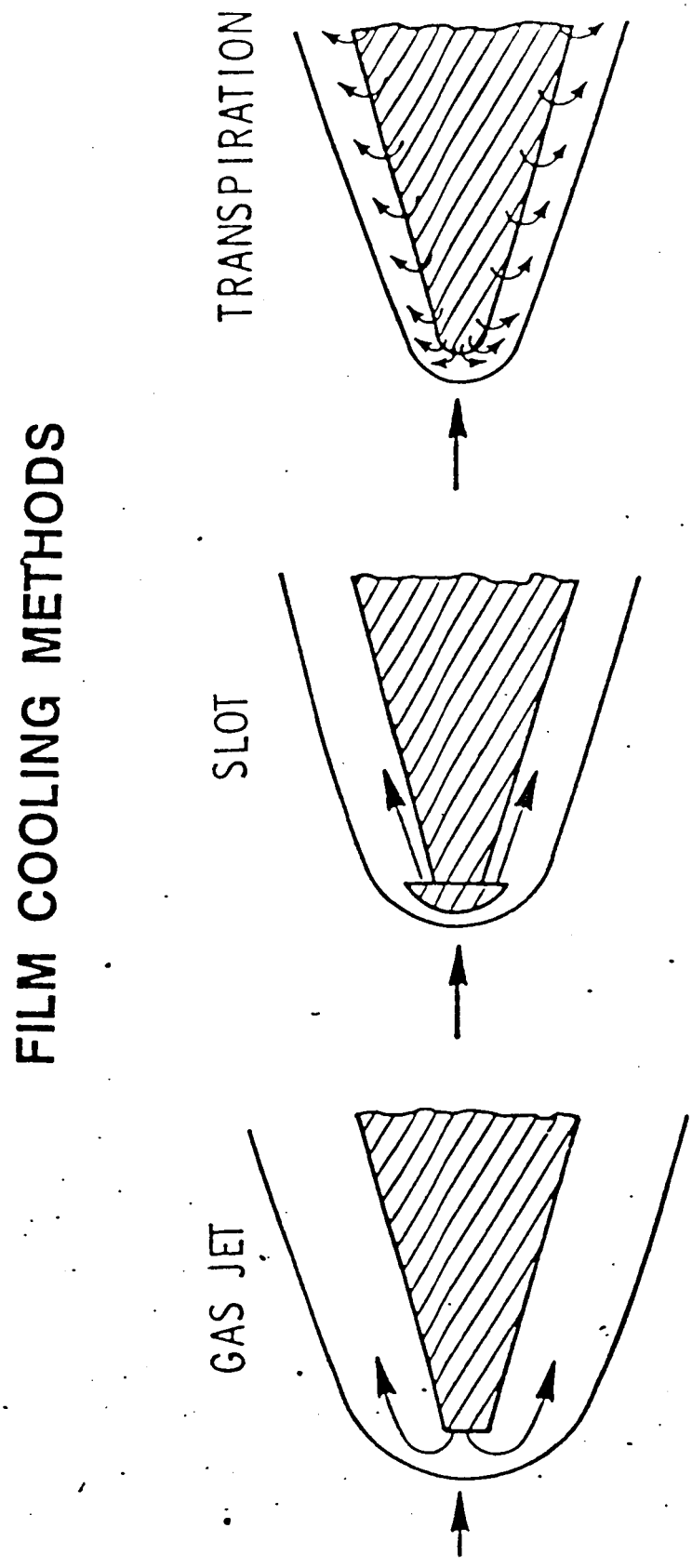

Figure 1. (Adapted from Reference 3.)

The studies conducted on film cooling by slot injection into a turbulent boundary layer can be divided into two main categories; A) Experimental studies and B) Analytical studies.

A. Experimental Studies

More experimental studies have been conducted when compared with analytical studies. Most of the experimental studies surveyed were investigations which measured surface properties needed to evaluate the effectiveness of slot injection film cooling of a surface for various geometric shapes. Hefner [9] measured the surface static pressures, equilibrium temperatures and skin friction downstream of a tangential slot injection. Parthasarathy and Zakkay [5] measured the heat transfer distributions downstream of a slot for various mass flow rates for a flat plate. Ko and Liu [10] also measured surface properties on a flat plate. These experimental results were compared with theoretical results.

Zakkay and Wang [11] studied multiple downstream tangential slot injection to investigate the film cooling effectiveness on the surface of a cone. By measuring the local adiabatic wall temperature, experimental results showed that film cooling effectiveness could be correlated. Zakkay et. al., [12] conducted an experimental investigation on slot cooling of a cylindrical body in a hypersonic main stream. Larue and Libby [13] analyzed the slot injection of helium into a turbulent boundary layer in air while Mironov et. al., [14] determined the minimum mass flow rate needed to displace the boundary layer away from the wall and the effects of free-stream turbulence on

heat transfer rates. Yu and Petrov [15] studied the heat transfer to the surface of a cone around which a hypersonic stream flows during the tangential injection of a fluid from slots.

Several of the experimental investigations reviewed involved determining optimum properties. Foster and Haji-Sheikh [16] investigated the heat transfer coefficients in the regions immediate downstream of the injection for inclined slots and inclined rows of holes. Best [17] conducted experiments to gain information on describing mathematically the effect of interaction between the tangential and normal coolant streams on the film cooling effectiveness and Cary and Hefner [18] as well as Richards and Stollery [19] investigated the effects of slot height and slot mass flow rate for a flat plate. In Eiswirth's et. al., [20] paper, the tangential slot gas film cooling of a tangential ogive configuration was tested. They varied the injection geometry and used several coolant gases. Hefner and Cary [21] took measurements of the surface equilibrium temperature downstream of swept slots with tangential air injection on a flat plate. Hefner, et al., [22] also studied a three-dimensional film cooling model with swept slots. A three-dimensional model was also used by Rastogi and Whitelaw [23] to measure the wall effectiveness downstream of film cooling slots.

Other experimental studies surveyed were conducted to gain insight into the mathematical model of a turbulent boundary layer with slot injection. Larue and Libby [24] took measurements in a turbulent boundary layer with slot injection of helium. Saad and Miller [25] experimental study indicated that very good correlation between experimental data and theory can be obtained.

B. Analytical Studies

The analytical studies reviewed showed that several finite-difference methods can be utilized to solve the conservation form of the flow equations. Plostins and Rubin [26] used the coupled block tridiagonal algorithm to evaluate the transverse momentum and continunity equations. A finite-difference model similar to Patankar and Spalding [27] was used for Metzger et. al., [28] to obtain measurements of profiles immediately downstream of a slot. Starkenberg and Creci [29] utilized Lin and Rubin's [30] method; a numerical technique used to solve the boundary layer equations with initial conditions reflecting mass injection. Beckwith and Bushnell [2] also presented a finite-difference method to calculate turbulent boundary layers with tangential slot injection. This method has been used by Cary et. al., [31, 32] to generate effectiveness data and good general agreement has been obtained with experimantal data.

The finite-difference method by Beckwith and Bushnell [2] was utilized in the present study to determine the heating rates to the surface of a cone-shaped body with tangential slot injection.

CHAPTER III

FORMULATION OF THE PROBLEM

The problem of heat transfer between a solid body and a fluid flowing pass is studied under rotation symmetry flow. Rotational symmetric flow in curvilinear coordinates, (x, y, θ), were given by White [33] where "x" represented the parallel distance measured from the nose to the body surface, "y" was the distance normal to the surface, and "θ" was the circumferential angle as indicated in figure 2. When the circumferential velocity called swirl is zero, the flow reduces to the special case of axisymmetric flow.

A cone-shaped body travelling at hypersonic speed experiences a large increase in the amount of heat being transferred to the surface of its body. The tangential slot and high speed trip the turbulent flow condition in the boundary layer. The complete form of the boundary layer equations which governs viscous flow are very difficult to solve. For turbulent flow, the equations are impossible to solve with present mathematical techniques because the boundary conditions become randomly time-dependent. The exact equations can be simplified using Prandtl's boundary layer approximations. By allowing the density, and thermal conductivity to be constant, the problem is specified completely by knowing the conditions for velocity, pressure and temperature at every point of the boundary of the surface in the flow.

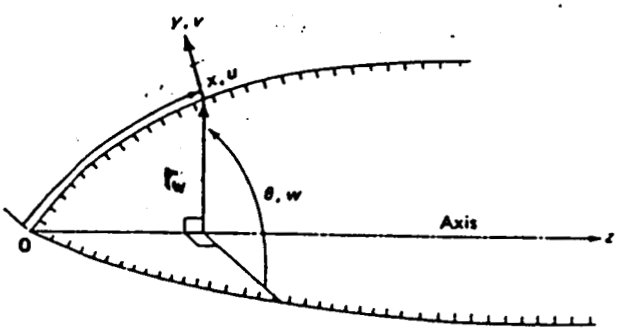

Figure 2. Coordinate System for Rotationally Symmetric Flow

The compressible turbulent boundary layer equations which governs a cone-shaped body with trangential slot injection are as follows:

The basic partial differential equations are

CONTINUITY:

$$\frac{\partial}{\partial x}(\rho u r) + \frac{\partial}{\partial y}(\rho V r) = 0 \qquad (2)$$

X-MOMENTUM:

$$\rho U \frac{\partial u}{\partial x} + \rho v \frac{\partial u}{\partial y} = \frac{-dP}{dX} + \frac{\partial}{\partial y}\left[\mu\left(1+\frac{\epsilon}{\mu}\right)\frac{\partial u}{\partial y}\right] \qquad (3)$$

TOTAL ENERGY:

$$\rho u \frac{\partial H}{\partial x} + \rho v \frac{\partial H}{\partial y} = \frac{\partial}{\partial y}\left\{\frac{\mu}{Pr}\left[\left(1 + \frac{\epsilon}{\mu}\frac{Pr}{Pr,t}\right)\frac{\partial H}{\partial y} - (1-Pr)\left(\mu\frac{\partial u}{\partial y}\right)\right]\right\} \qquad (4)$$

All flow quantities in the above equations are time-mean values. To account for the tangential slot injection of a homogeneous gas, the conservation of species equation is calculated.

For no chemical reactions, the species equation becomes

$$\rho u \frac{\partial g}{\partial x} + \rho v \frac{\partial g}{\partial y} = \frac{\partial}{\partial y}\left[\left(\frac{\mu}{Sc} + \frac{\epsilon}{Sc,t}\right)\frac{\partial g}{\partial y}\right] \qquad (5)$$

where g is the ratio of local to edge concentration of species, i, that is,

$$g = \frac{C_i}{C_{i,e}} \qquad (6)$$

The boundary conditions for equation 5 are

$$y = 0 \quad \text{for} \quad \left(\frac{\partial g}{\partial y}\right) = 0 \tag{7}$$

$$y = y_e \quad \text{for} \quad g = 1 \tag{8}$$

In the present study, equations 2,3,4 and 5 were solved using a computer program that calculated by a finite-difference method the turbulent boundary layers with tangential slot injection. In the computer program, the concentration of a foreign specie represented the behavior of a trace specie mixed with air. The following assumptions are made -

1. The flow is axisymmetric flow
2. Tangential fluid injection
3. dP/dy = 0; the change in pressure in the "Y" direction is zero. This is valid for matched pressure condition.
4. Thin slot lip compared with boundary layer thickness.

The turbulent terms appearing in the conservation equations were modeled using the mixing length hypothesis. The turbulent stress term, τ_t, occurring in the mean flow equation (Eq. 3) is given as

$$\tau_t = \varepsilon \frac{\partial u}{\partial y} \tag{9}$$

Using the mixing length hypothesis, the turbulent shear stress is given as -

$$\tau_t = \rho \ell^2 \left| \frac{\partial u}{\partial y} \right| \frac{\partial u}{\partial y} \tag{10}$$

where "ℓ" is defined as the mixing length.

The turbulent prandtl number, $P_{r,t}$, appearing in the total energy equation (Eq. 4) was formulated by modeling the eddy conductivity, κ. Modeling the eddy conductivity resulted in the following definition for the turbulent prandtl number.

$$P_{r,t} = \frac{C_p \varepsilon}{\kappa} \tag{11}$$

The mixing length model used in the program is given in [31]. Algebraic length scales are used to describe the mixing length distribution in three major zones. The three zones are defined downstream of the slot and are discussed individually. Zone I is physically the near-slot region in which can be distinguished the pure injectant flow region, the embedded boundary layer injectant mixed flow region and the pure boundary layer flow region. In Zone II, the mixing has engulfed the pure injectant flow such that only the mixed flow and pure boundary layer flow regions are distinguishable. In Zone III, the mixed flow region is nearing the boundary layer edge, and the flow is considered fully mixed. The mixing zones along with illustration of the length scales are shown in figure 3. A complete discussion of the philosophy and structure of turbulence modeling for slot flows is presented in [2] and [34].

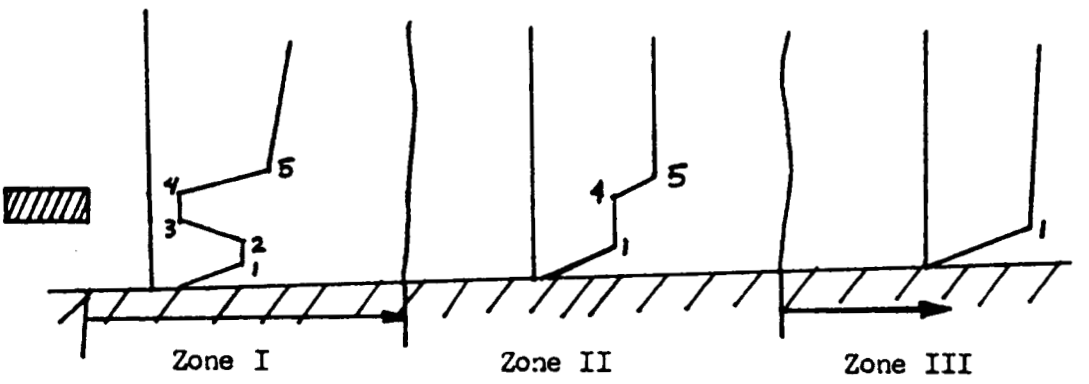

Figure 3. Mixing Length Profiles for a Typical Slot Injection Flow Showing the Three Major Zones

CHAPTER IV

NUMERICAL PROCEDURE

The numerical method solves the partial-differential equations for the mean motion of an axisymmetric, compressible turbulent boundary layer with tangential injection by an implicit finite-difference procedure.

In order to keep the number of steps across the boundary layer (in the y-direction) approximately constant and to take advantage of similar profile shapes which exist for certain conditions, a similarity transformation of "x" and "y" were introduced. The system of equations, that is, Equations 2 - 5, were transformed using the similarity transformations for "x" and "y" and solved by an implicit finite-difference procedure. A sample grid and the node notation is illustrated in figure 4. The step size in the "y" direction was varied as well as the step size in the"x" direction. The solution is advanced downstream in the "x" direction by redefining the m = 2 values as m = 1 values and a new m = 2 station is chosen a distance downstream. The two point difference scheme in the "x" direction was used.

The input data is specified at m = 1 for n = 1 to n = n_{max} from which values of all variables are to be computed at the next station (m = 2). The various derivatives in the transformed equation are replaced by linear difference equations and the equations are evaluated at an intermediate station. Complete details of the numerical procedure and the computer program are given in [2] and [35].

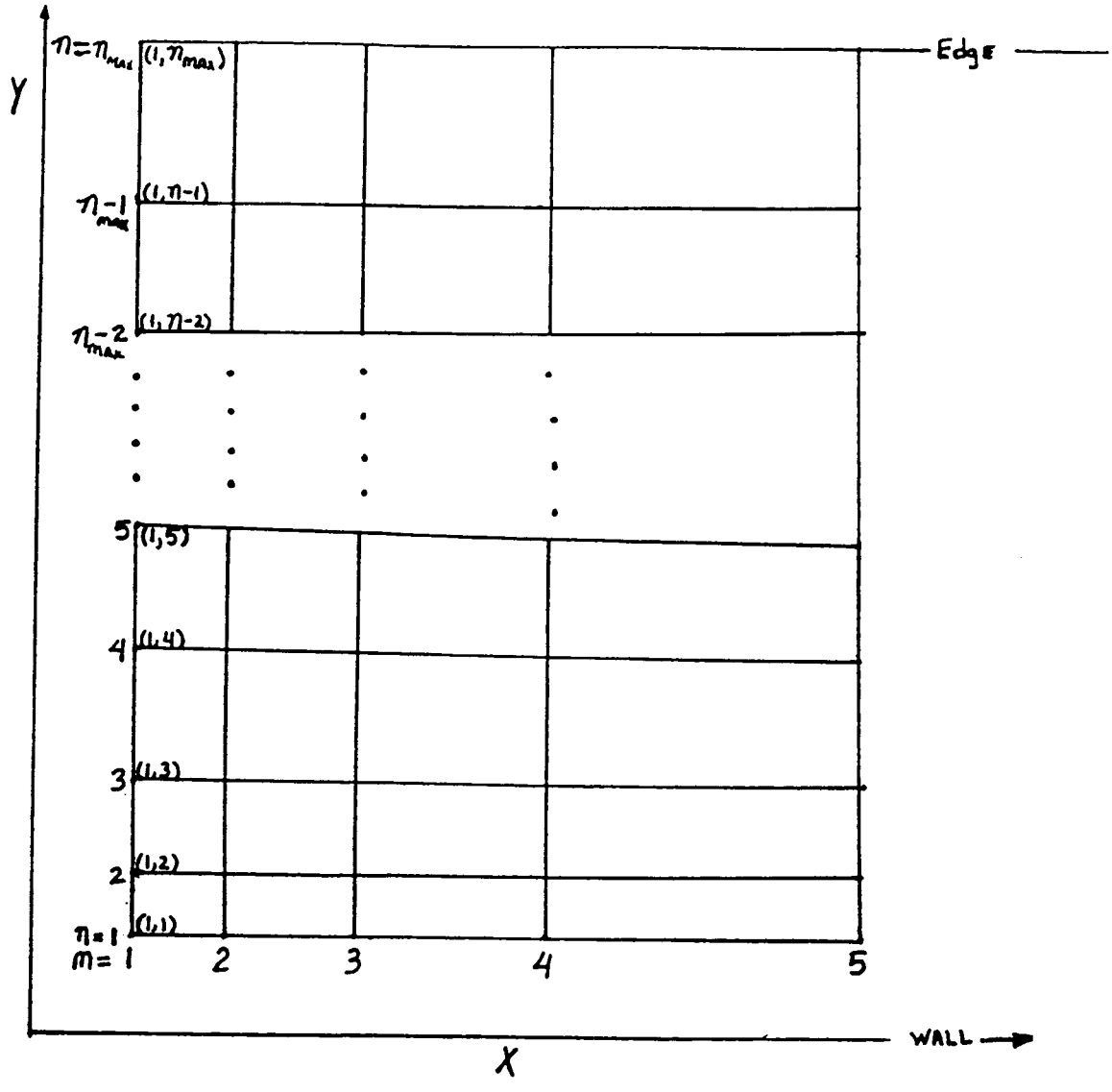

Figure 4. Grid Notation

CHAPTER V

NUMERICAL RESULTS

A 12.5 degree half angle cone with three different nose shapes was film cooled in a 8 foot temperature tunnel at NASA Langley (see Figure 5). The nose shape studies in this paper was the 3 inch radius tip with two tangential slots (see Figure 6). The 83.3 inch cone was travelling at a Mach speed of 6.95 with a free-stream unit reynolds number of 1.18×10^6/ft. The cone was positioned at an angle of attack of zero degree and nitrogen was injected from the slots. The input file needed as boundary conditions in the computer program was developed using preliminary data obtained from NASA (see Appendix A and Appendix B).

The velocity profile used in the input file was calculated using the equations for turbulent flow in a duct for the slot and the $1/7^{th}$ power law for the free-stream flow over a flat plate. The total enthalpy profile was then calculated using the velocity profile. The velocity and enthalpy profiles used in the computer program are shown in figures 7 and 8 for a velocity ratio of 0.2.

The radius of curvature of the nose cone was calculated using the downstream distance as given in Equations 12 and 13.

$$r_w = 3 \sin\left(\frac{x}{3}\right), \quad x \leq 4.71 \text{ inches} \tag{12}$$

$$r_w = 3 + 0.2217x, \quad x > 4.71 \text{ inches} \tag{13}$$

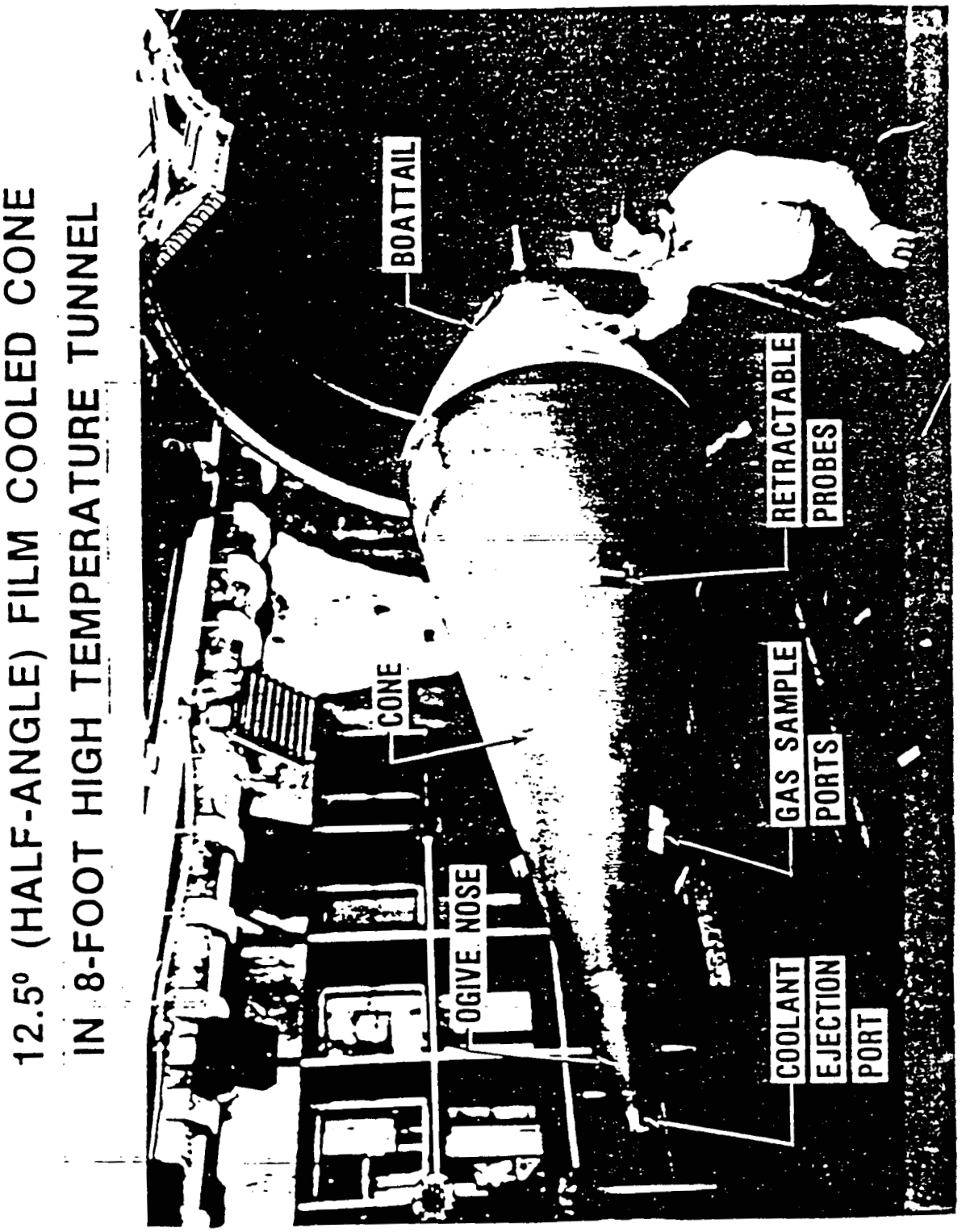

Figure 5. (Adapted from Reference 3.)

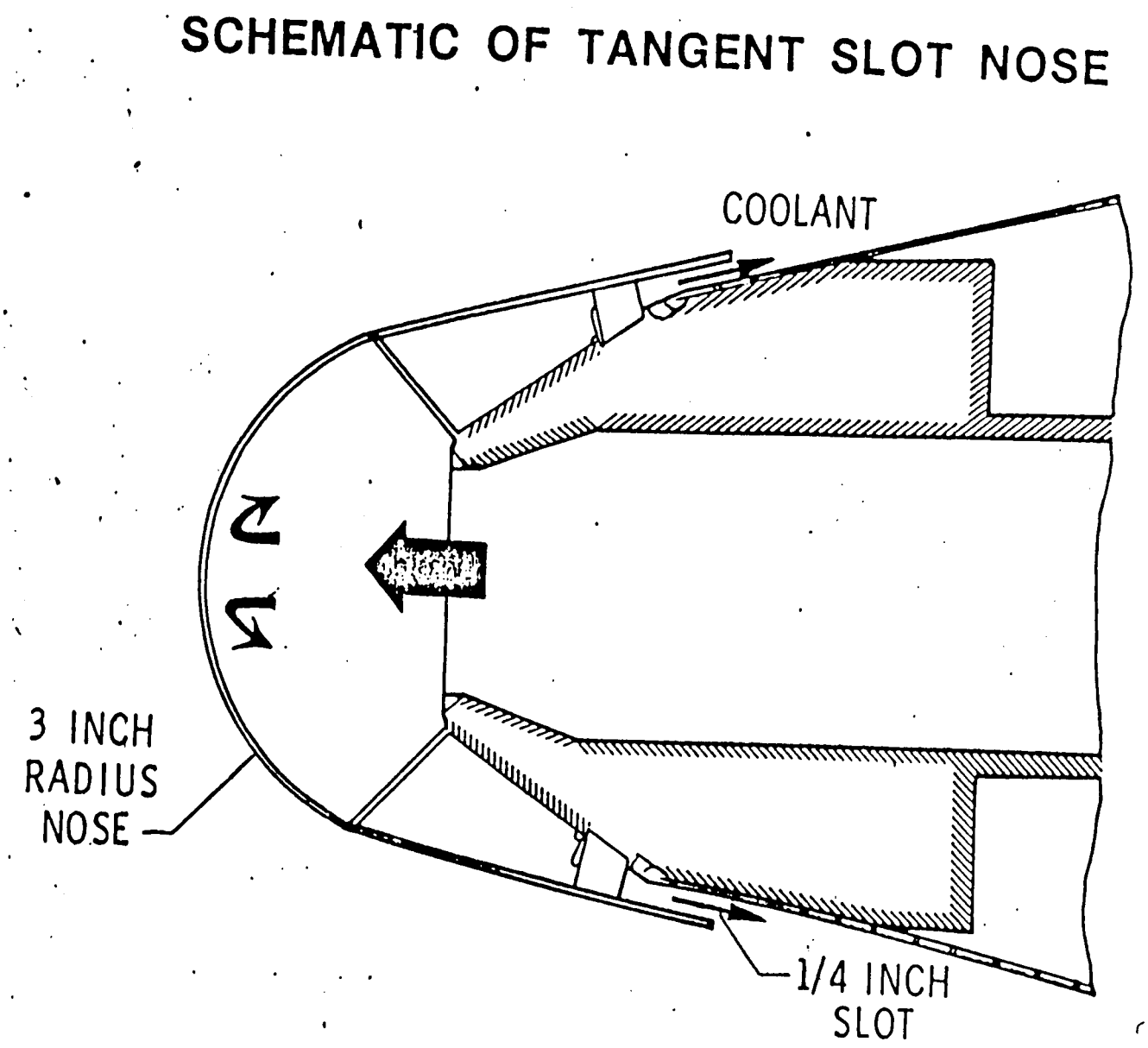

Figure 6. (Adapted from Reference 3.)

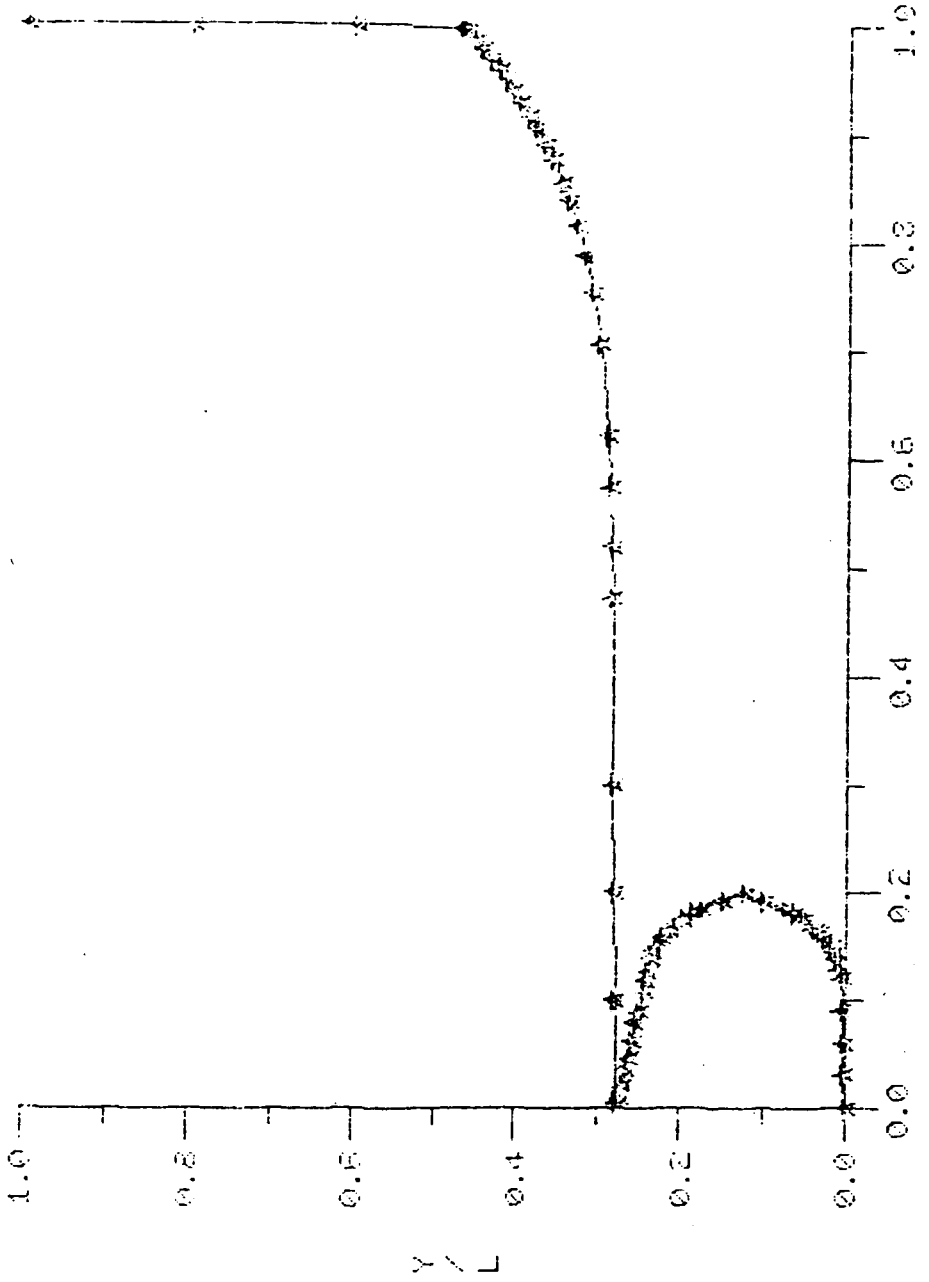

Figure 7. Initial Velocity Profile for Velocity Ratio = 0.2

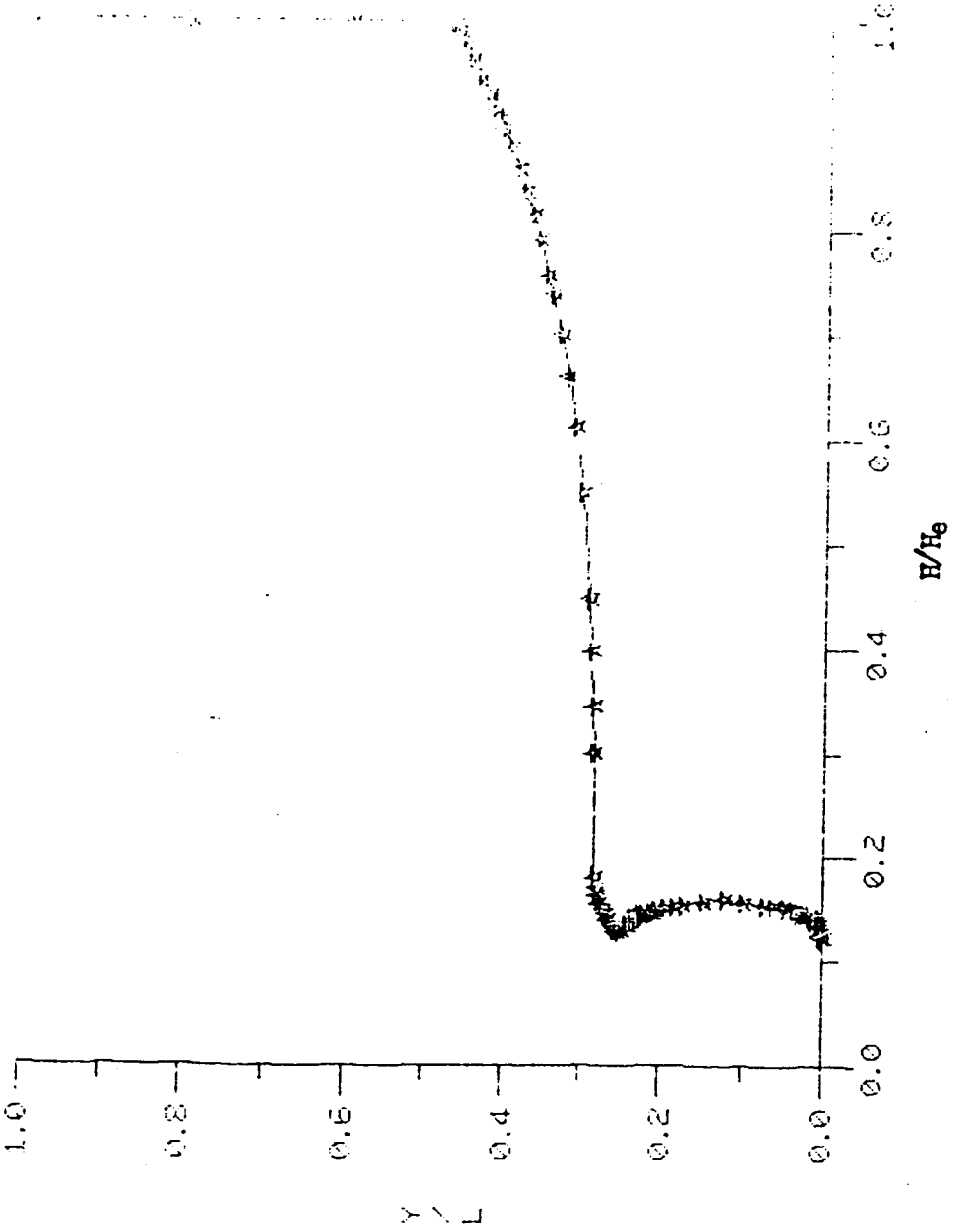

Figure 8. Initial Enthalpy Profile for Velocity Ratio = 0.2

As a general case, the results for the slot to free-stream velocity ratio of 0.2 are discussed in detail. The velocity, temperature, Mach number, stagnation temperature, stagnation pressure and the heat transfer rate profiles were obtained from the numerical methods developed by Beckwith, and Bushnell [2]. The profiles were analyzed to determine what happened in three major regions; the near-slot region, the mixing region and the fully mixed region.

In the near-slot region, it is possible to distinguish the pure injectant flow region, the embedded boundary layer-injectant mixed flow region and the pure boundary layer flow region. In the mixing region, the pure injectant flow has been engulfed and only the mixed flow and pure boundary layer flow regions exist. In the fully mixed region, the boundary layer is fully developed.

Figure 9 gives the concentration profiles for velocity ratic of 0.2 at dimensionless downstream distances of 8.0, 9.1, and 18.0. The concentration distribution for air at 99% and 1% are also given. The beginning of the mixing region can be observed. The point where mixing begins is in good agreement with the results obtained by Cary, Bushnell, and Hefner [31]. Their results show that the mixing region occurs at a downstream distance on the order of magnitude of 10 inches. The results shown in figure 9 gives a downstream distance of approximately 9.3 inches.

A. Velocity Profiles

The general picture of the flow which developed can be seen in figures 10a - d. These results are normalized with respect to the

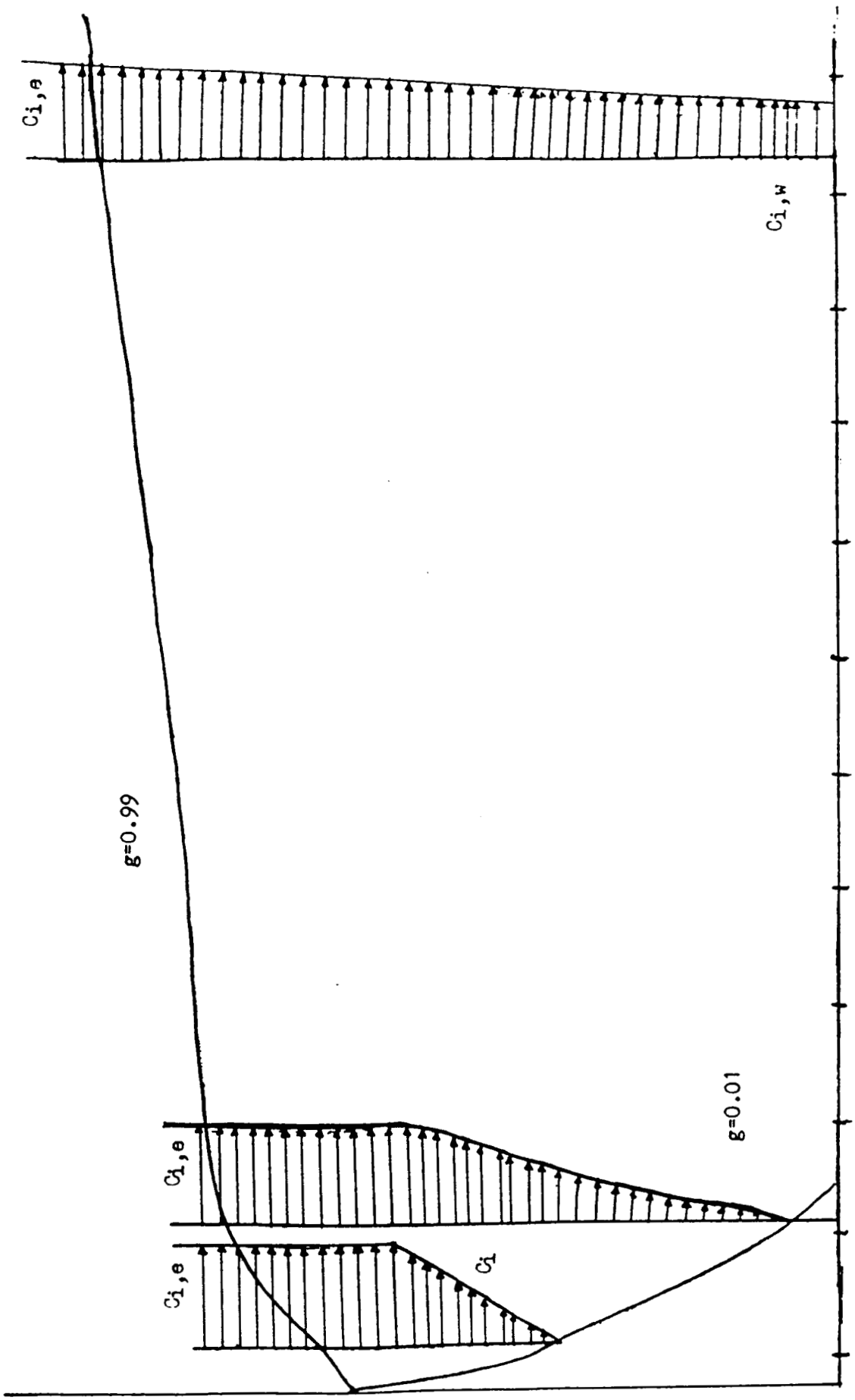

Figure 9. Concentration Profile for Velocity Ratio = 0.2

free-stream velocity, u_e. The initial velocity profile was that of a turbulent pipe flow of pure nitrogen underneath a fully developed turbulent boundary layer of air over a flat plate. Beginning at the slot exit location of x = 7.73 inches, the velocity distribution indicated the formation of a turbulent pipe flow which disintegrated with increasing distance along the surface of the cone. This zone ranging from $7.73 < x < 9.3$ inches is the near slot region as shown in figure 10 a - b. At a distance of 9.3 inches along the surface of the cone, the velocity profile revealed that the free-stream air had engulfed the pure injectant flow such that only the mixed flow and pure boundary layer regions were distinguishable. Thus the zone ranging from $9.3 < x < 26.3$ inches established the mixing region. The beginning of the mixing zone is defined to be the point where the wall concentration is 1% while the end of the mixing zone is defined as the point where the wall concentration is 85%. A typical profile of the mixing region is shown in figure 10 c. Note that the velocity profile was nearly linear in this region. Farther downstream of the slot, the profile had the characteristic of a boundary layer fully recovered to the no injection profile and the flow was considered fully mixed. Figure 10 d gives an example of a profile in the fully mixed region.

B. Temperature Profiles

The temperature profiles at various locations on the surface of the model have been plotted in figures 11 a - d. These results are normalized with respect to the free-stream temperature, t_e. The initial temperature profile as shown in figure 11 a was evaluated in the

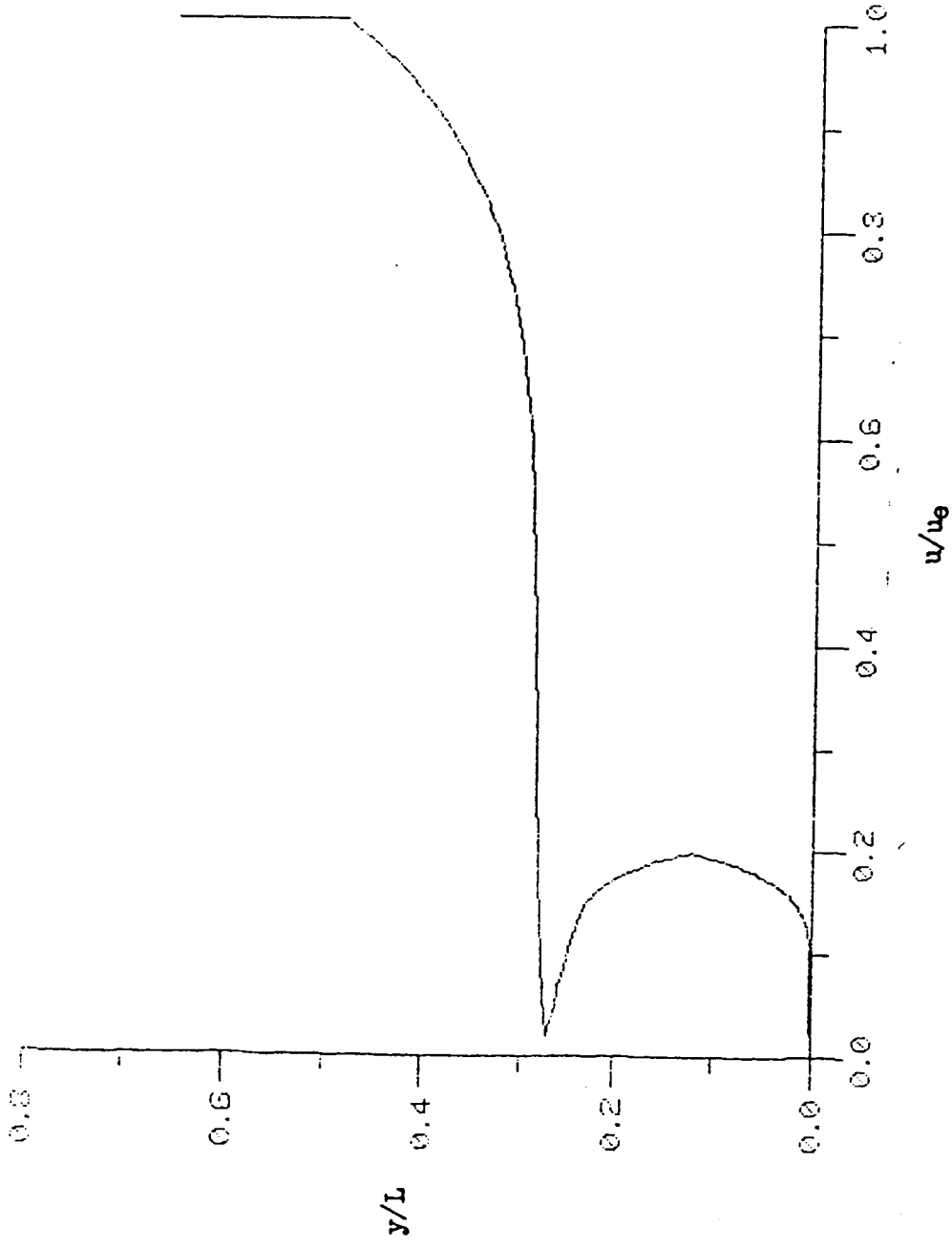

Figure 10a. Velocity Profile at x=7.73

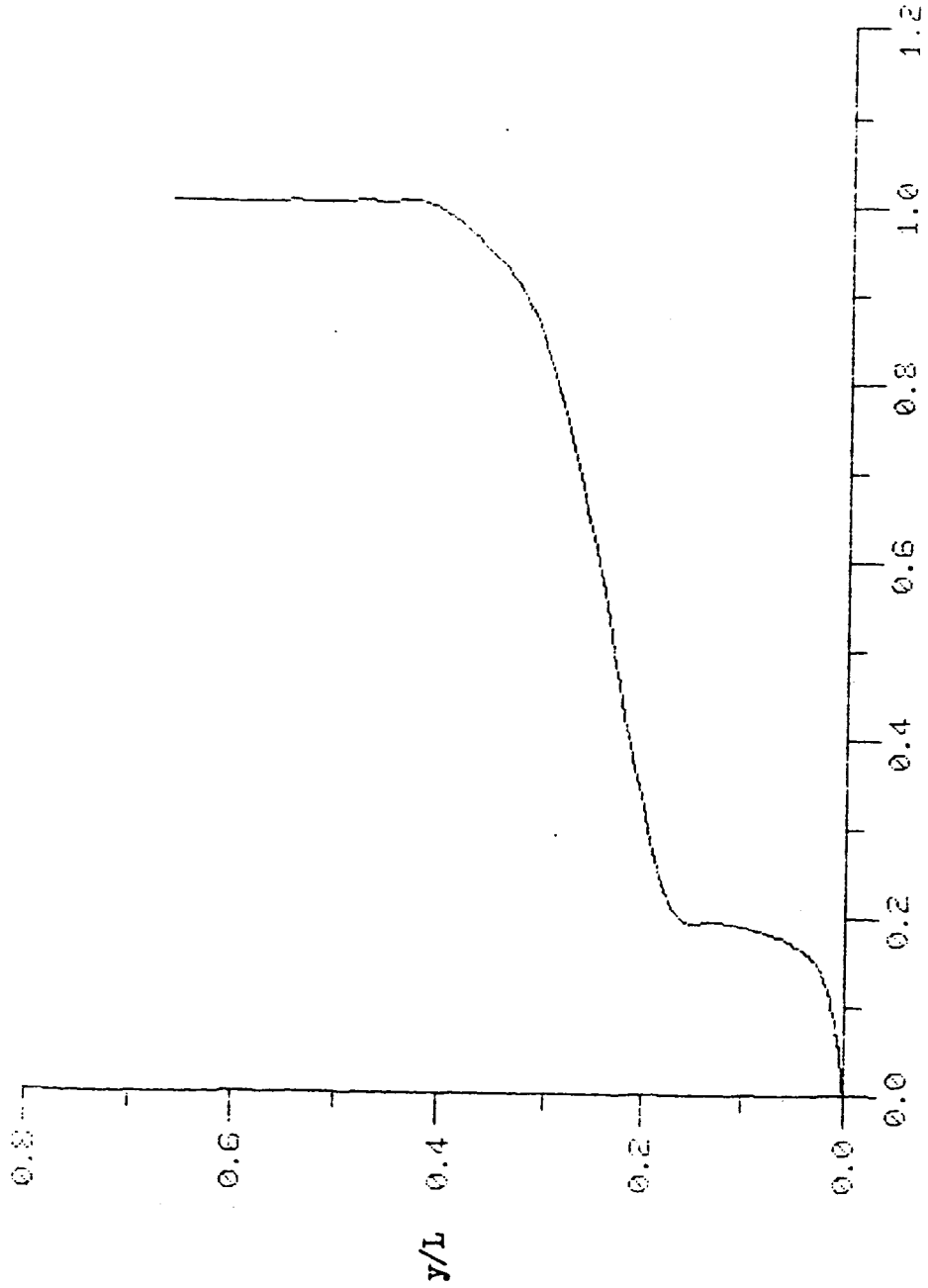

Figure 10b. Velocity Profile at x=8.0

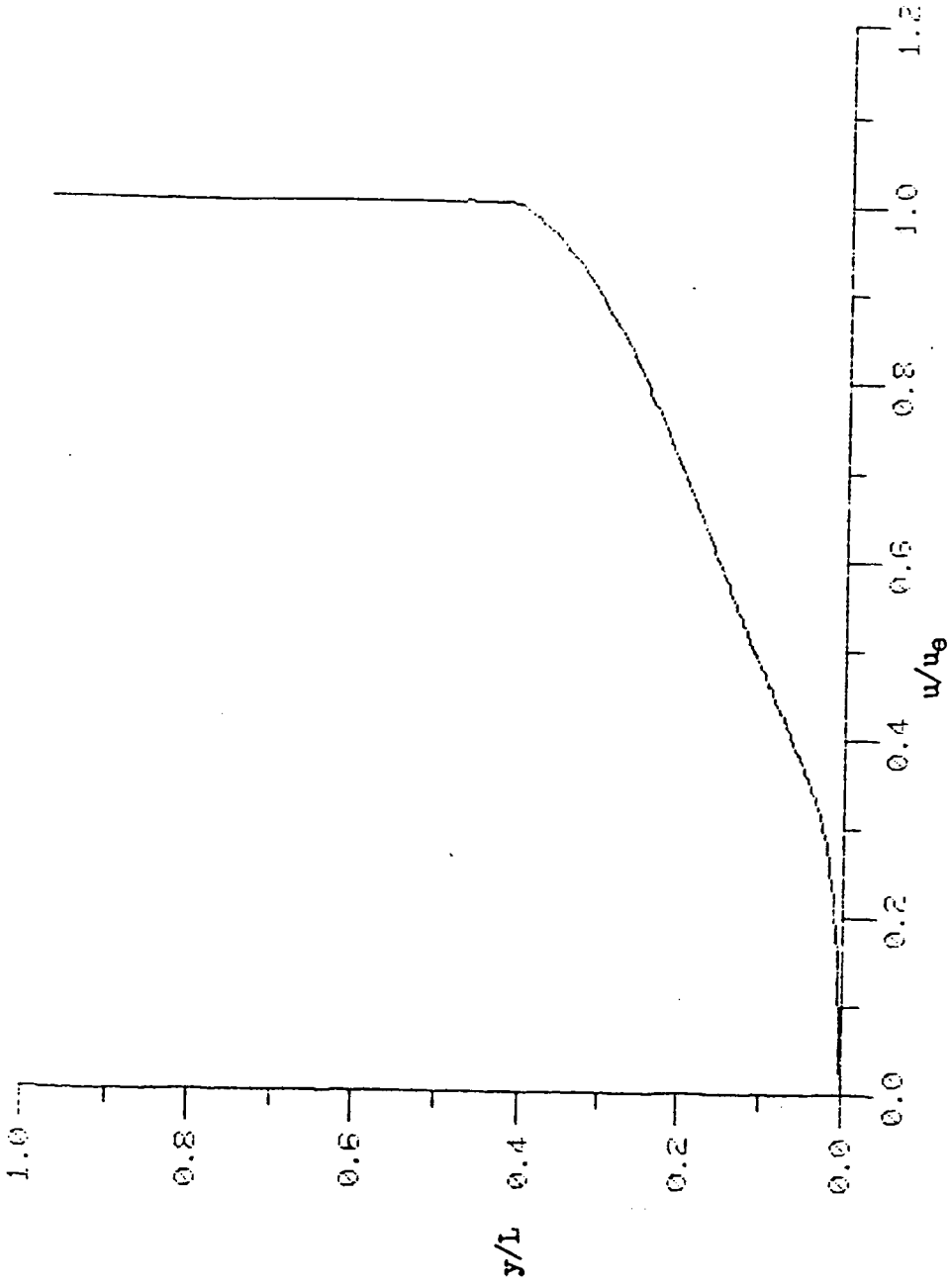

Figure 10c. Velocity Profile at x=12.01

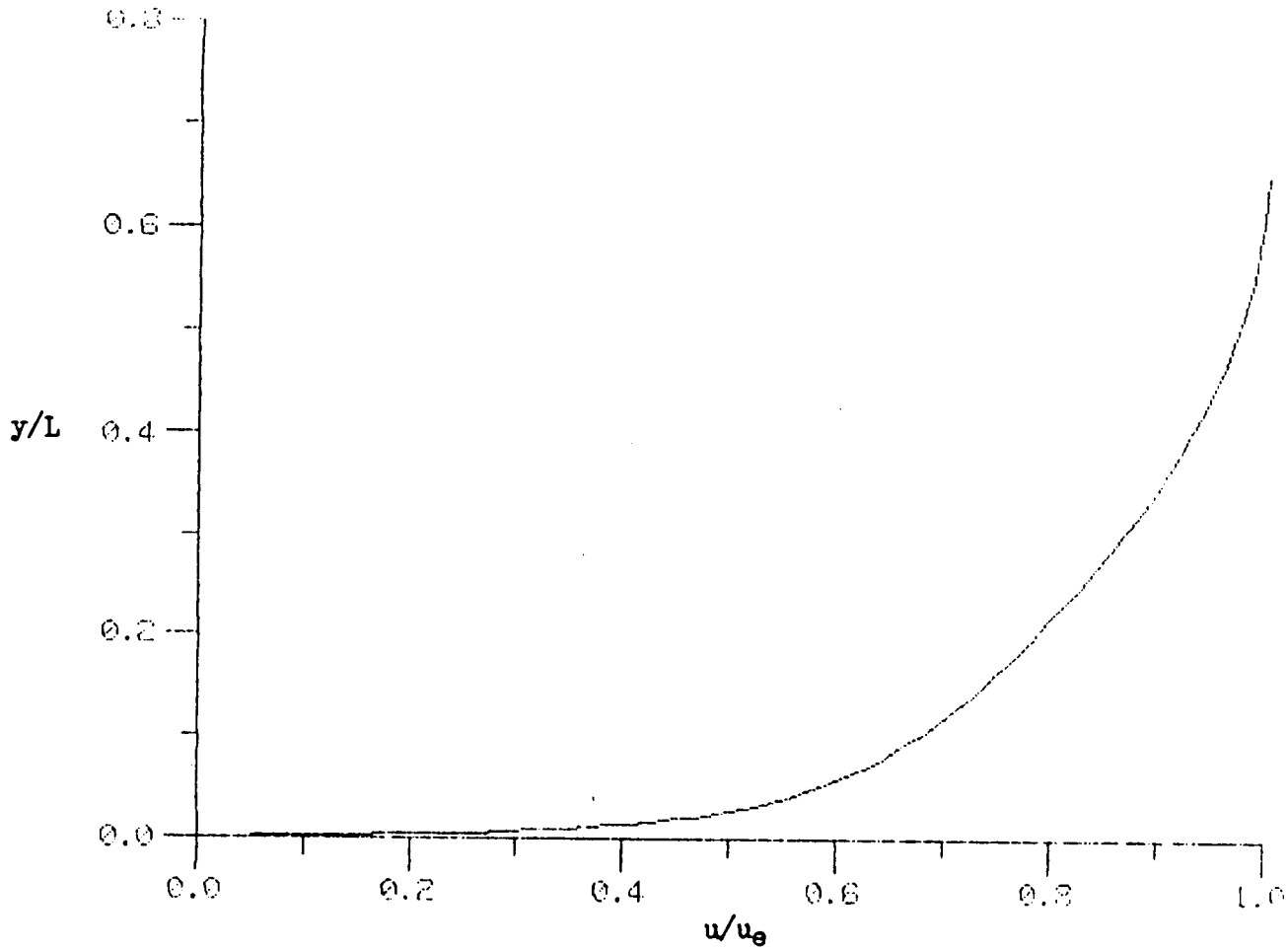

Figure 10d. Velocity Profile at x=40.03

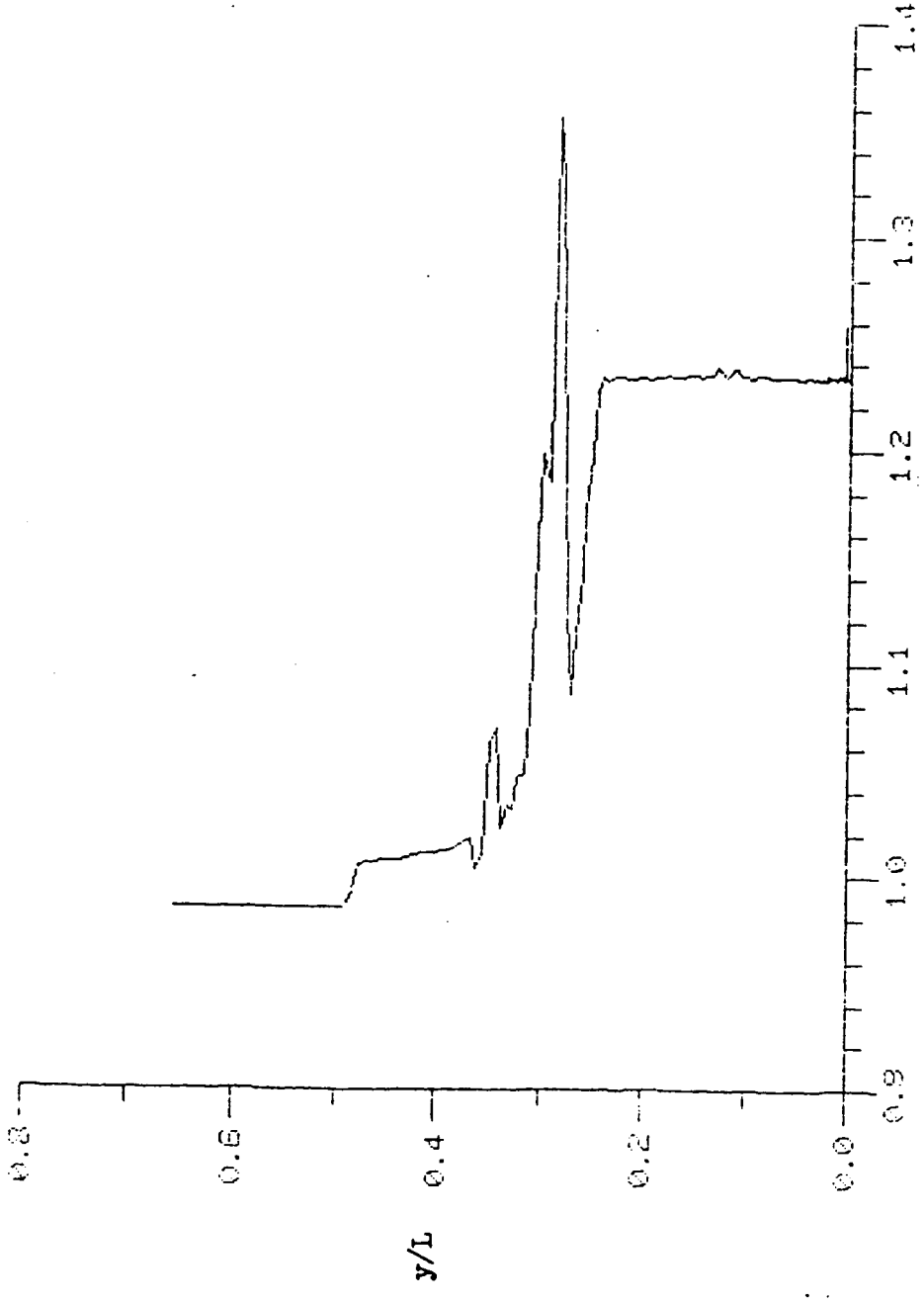

Figure 11a. Temperature Profile at x=7.73

computer programming from the input velocity profile and the enthalpy profile. The temperature distribution inside the slot as well as that above the slot lip region was constant. In the slot lip region, however, the temperature appeared to be unstable. It is in this region that the flow transitioned from nitrogen at constant properties to air at constant properties. The air is basically turbulent layer flow so the temperature profile approaches that of a fully developed profile for heat transfer to the surface of a flat plate.

As the distance along the surface of the model increases, the temperature inside the slot remains constant and the temperature distribution in the slot lip region showed that it was being affected by the free-stream temperature above the slot lip region. The profile in the slot lip region as seen in figure 11b was that of heat transfer to the nitrogen gas.

Proceeding farther away from the slot exit, the mixing region is established. The constant temperature distribution inside the slot has been completely replaced by the hotter temperature in the free-stream as shown in figure 11c. The temperature distribution indicated a profile for heat transfer to the gaseous mixture as well as to the surface of the model. Proceeding even farther downstream from the slot exit, the fully developed region was encountered. The boundary layer thickness increased and the temperature distribution of figure 11d was that of a fully developed profile for heat transfer to the surface of a nose cone.

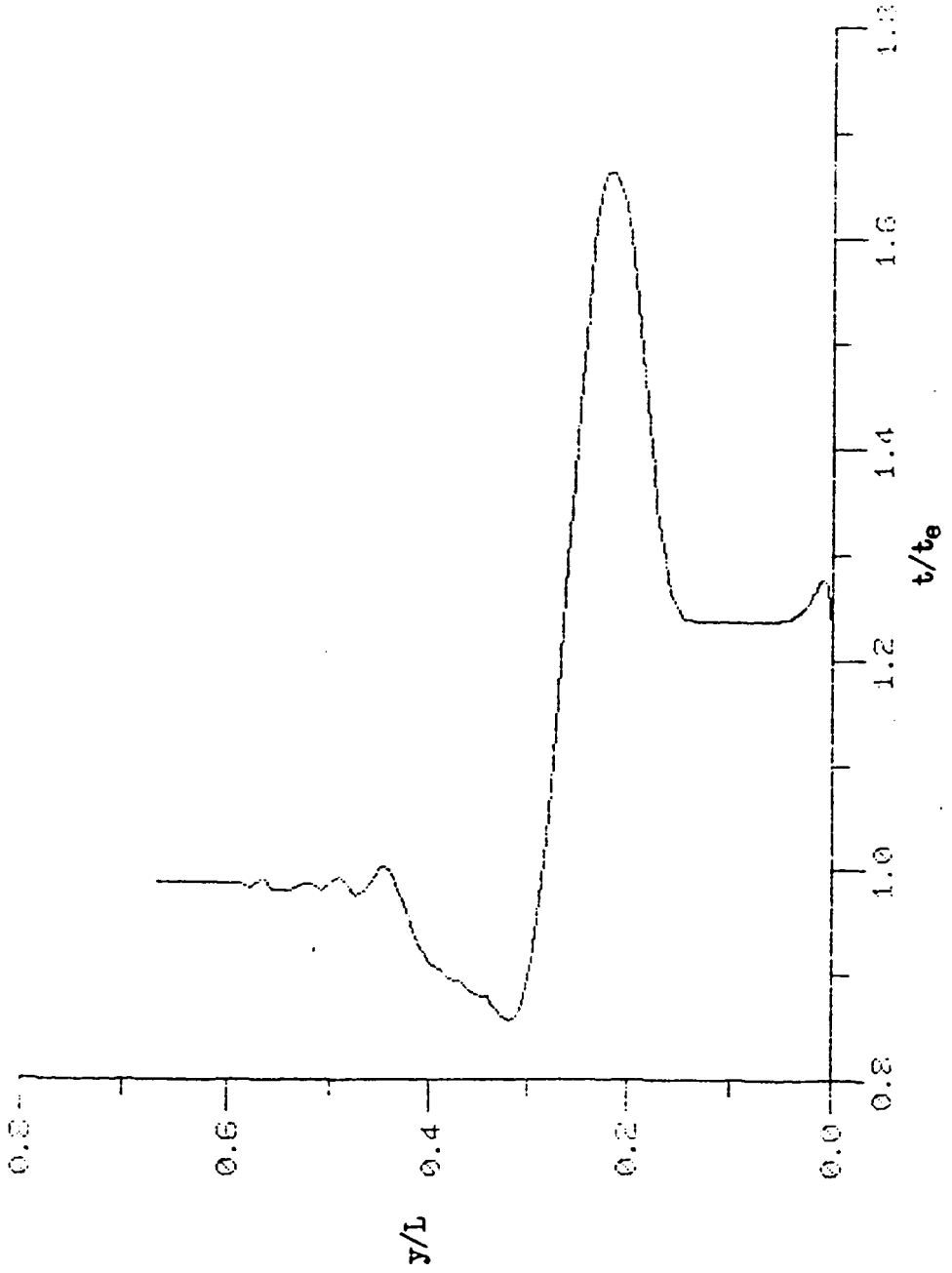

Figure 11b. Temperature Profile at x=8.0

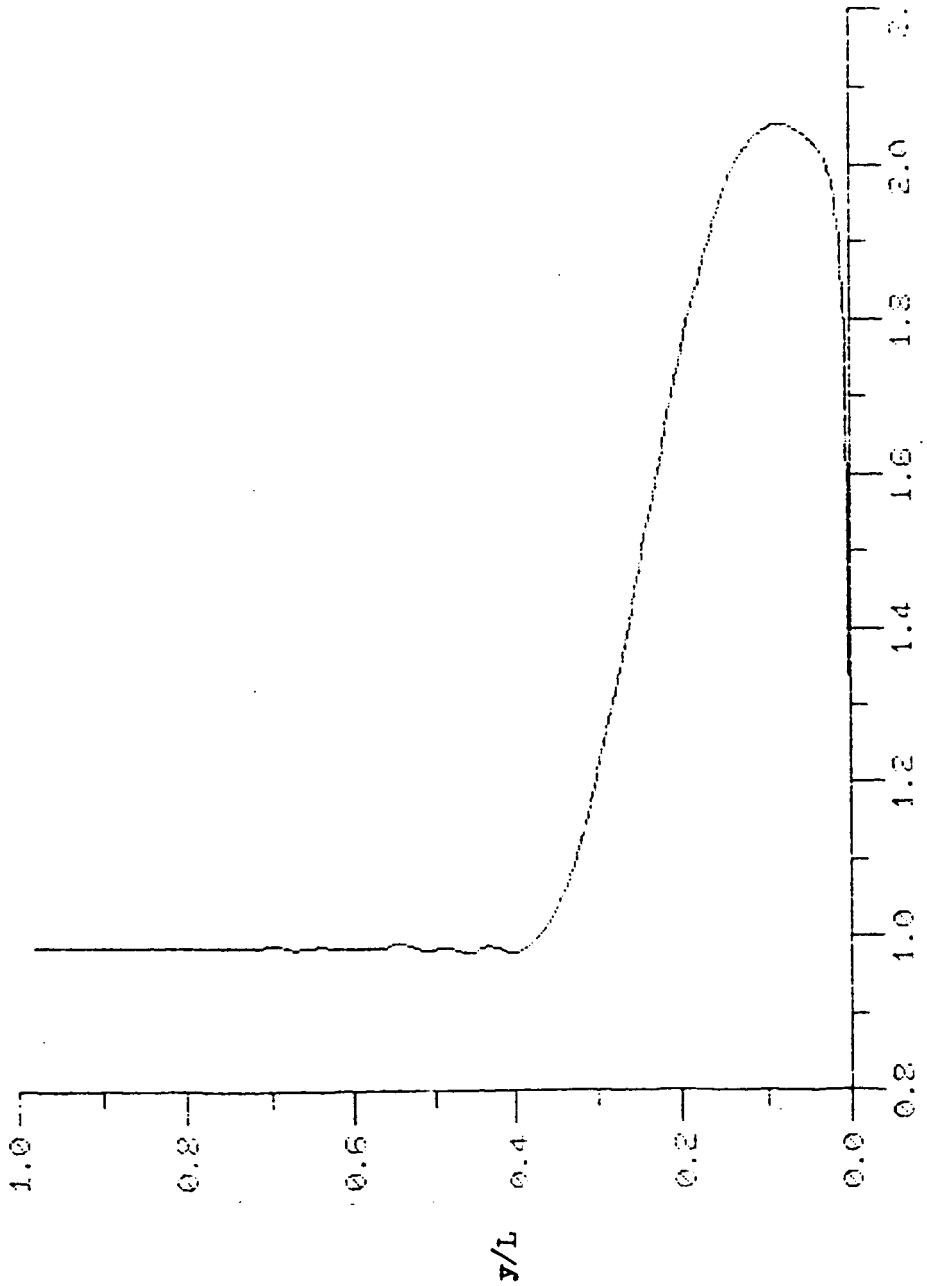

Figure 11c. Temperature Profile at x=12.01

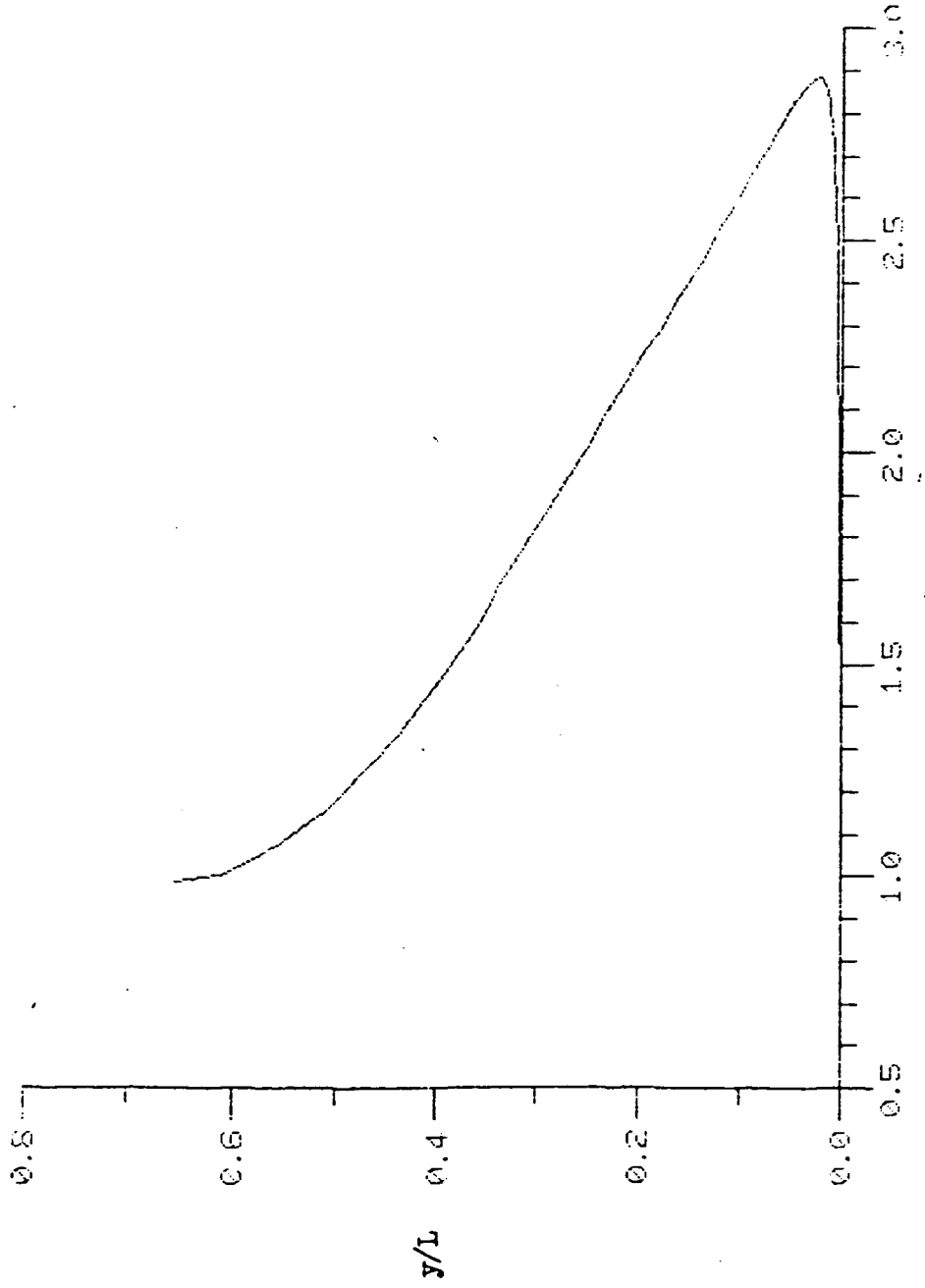

Figure 11d. Temperature Profile at x=40.03

C. Mach Number Profiles

The Mach number profiles at various locations on the surface were plotted in figures 12a - d. Initially the Mach number distribution was very similar to the velocity distribution which represents a turbulent pipe flow profile of pure nitrogen underneath a fully developed turbulent boundary layer of air over a flat plate. This can be observed in figure 12a. Farther away from the slot exit but still in the near slot region, see figure 12b, the turbulent pipe flow profile begins to disintegrate. The velocity distribution primarily dominated the Mach number distribution except above the slot's lip thickness. Above the slot's lip thickness area the Mach number distribution was affected primarily by the temperature distribution. In the mixing region, farther downstream of the slot, the turbulent pipe flow profile was no longer present as shown in figure 12c. The effects of the velocity and temperature distributions were felt throughout the Mach number profile. Farther downstream of the slot exit in the fully mixed region, the boundary layer thickness had increased and the Mach number distribution was affected by the velocity and temperature distributions primarily. Figure 12d is a typical example of the Mach number distribution in the fully mixed region.

D. Stagnation Temperature Profiles

The stagnation temperature profile at various locations on the surface of the model were plotted. The initial profile was dominated by the Mach number. For the near slot region, figure 13a and figure 13b showed that the stagnation temperature was nearly constant since the

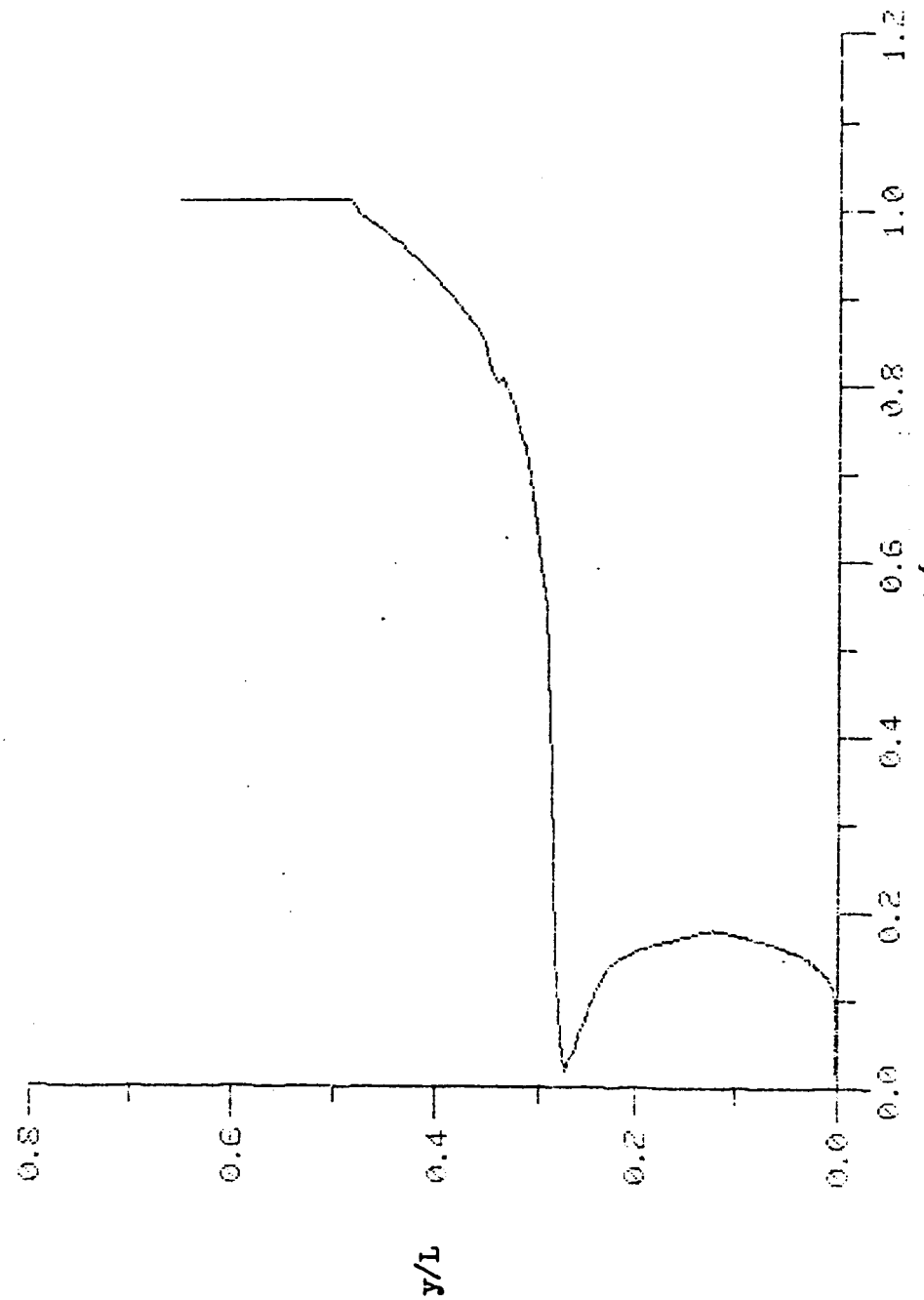

Figure 12a. Mach Number Profile at x=7.73

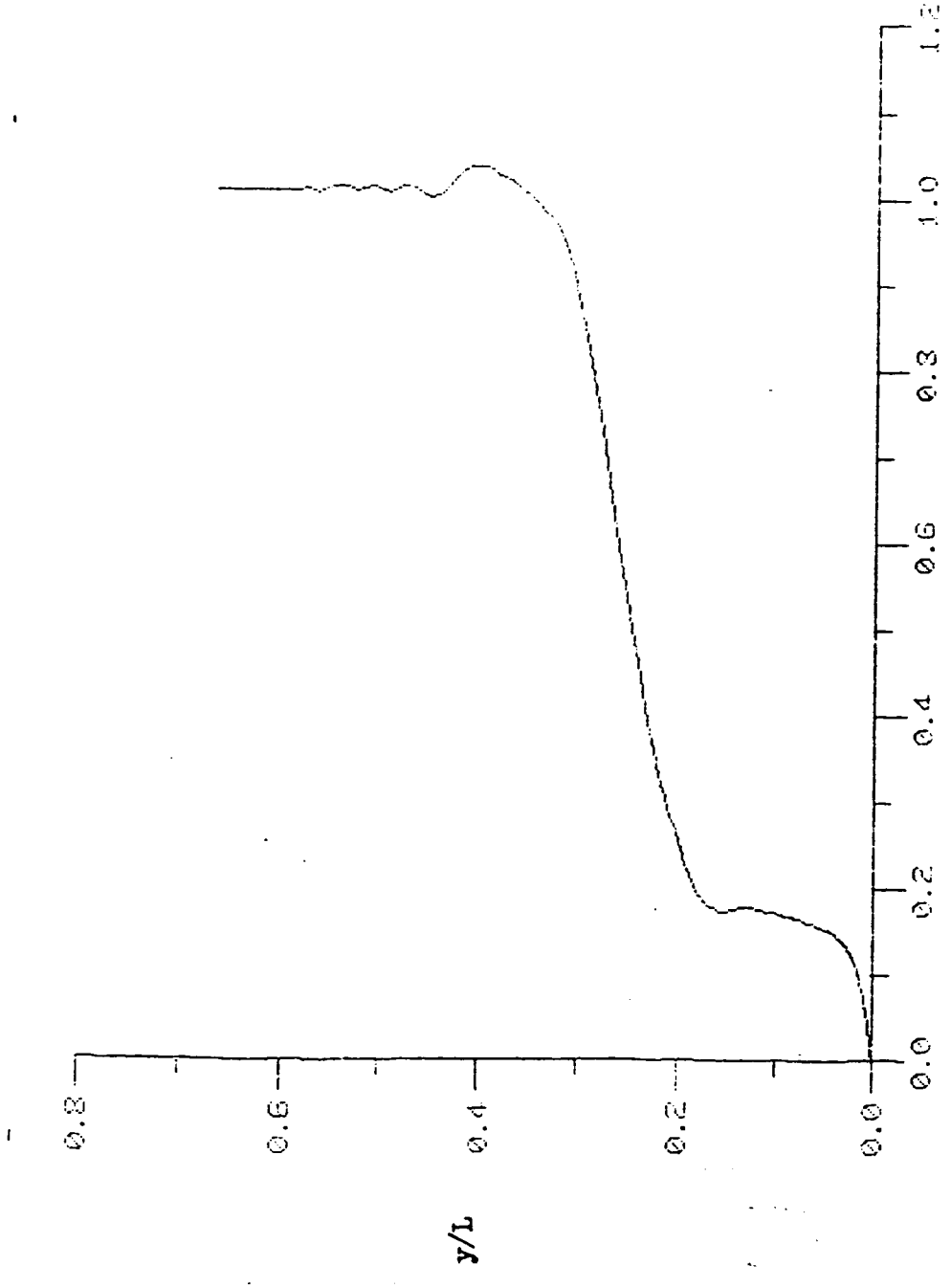

Figure 12b. Mach Number Profile at x=8.0

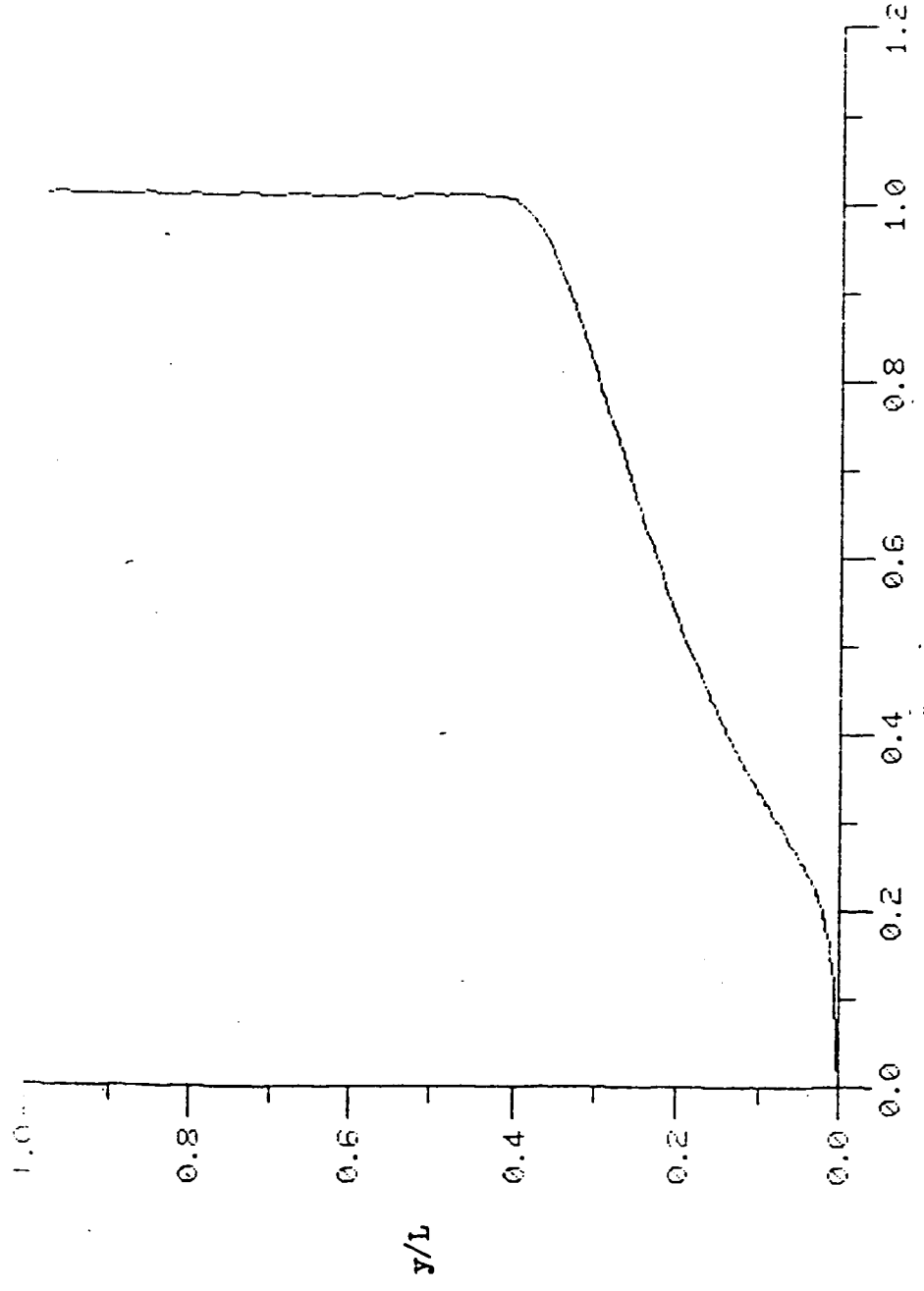

Figure 12c. Mach Number Profile at x=12.01

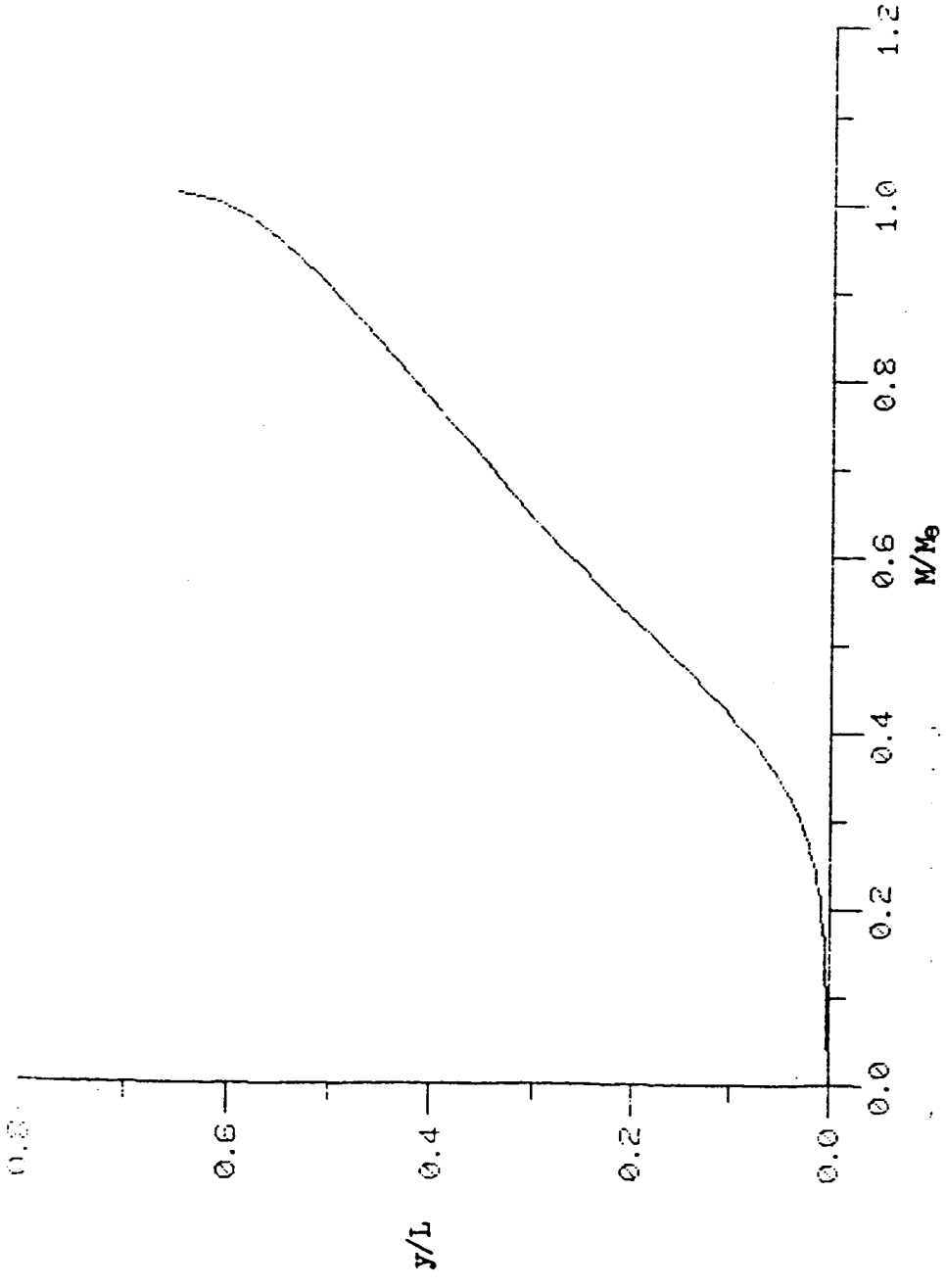

Figure 12d. Mach Number Profile at x=0.03

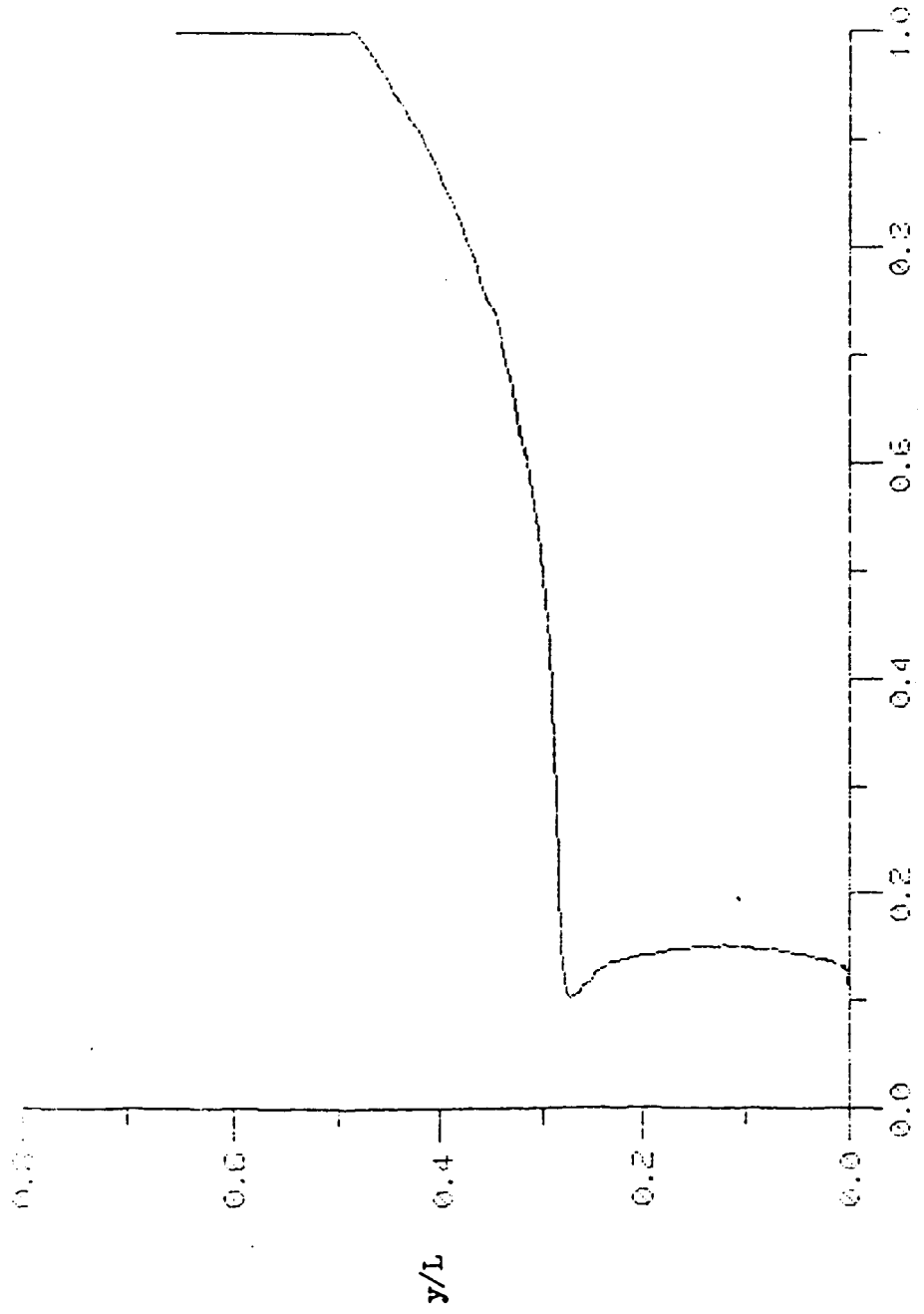

Figure 13a. Stagnation Temperature Profile at x=7.73

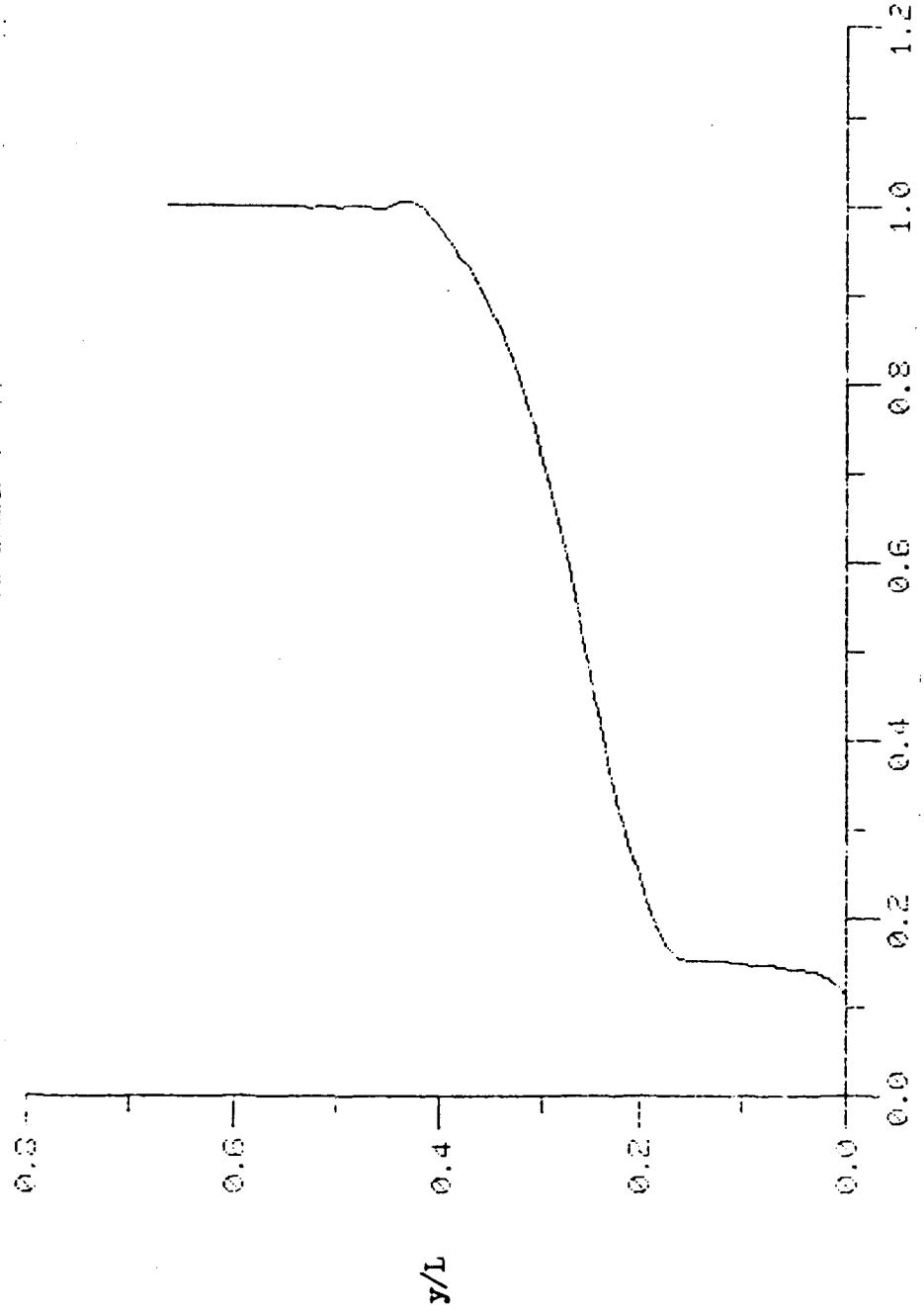

Figure 13b. Stagnation Temperature Profile at x=8.0

Mach number in that region was approximately unity. Proceeding downstream of the slot exit, the profile in the lip area begins to move closer to the surface of the body. Figure 13c showed that the constant profile inside the slot was eventually replaced with a linear stagnation temperature profile. In the fully mixed region, the Mach number at the wall was zero and the stagnation temperature inside the slot region was dominated by the temperature distribution. Since the velocities were large, the kinetic energy term dominated over the enthalpy term away from the wall. Therefore, the stagnation temperature profile was similar to the velocity profile as shown in figure 13d.

E. Stagnation Pressure Profiles

Inside the slot, the stagnation pressure ratio appeared to be zero. Actually the slot's Mach number was approximately unity and the stagnation pressure ration was very small at sonic flow. In the region above the slot, the stagnation pressure profile was linear. The linearity occurred because the stagnation pressure was proportional to the velocity raised to the 7th power. When the velocity was calculated using the 1/7th power law, the stagnation profile became linear as seen in figure 14a. Farther away from the slot's exit, the pure boundary layer flow region increased the velocity in the mixed flow region. The higher velocity increased the Mach number causing the stagnation pressure to increase. Proceeding farther downstream, the high velocity in the pure boundary layer flow region propagated to the surface of the model as can be observed in figure 14b and figure 14c.

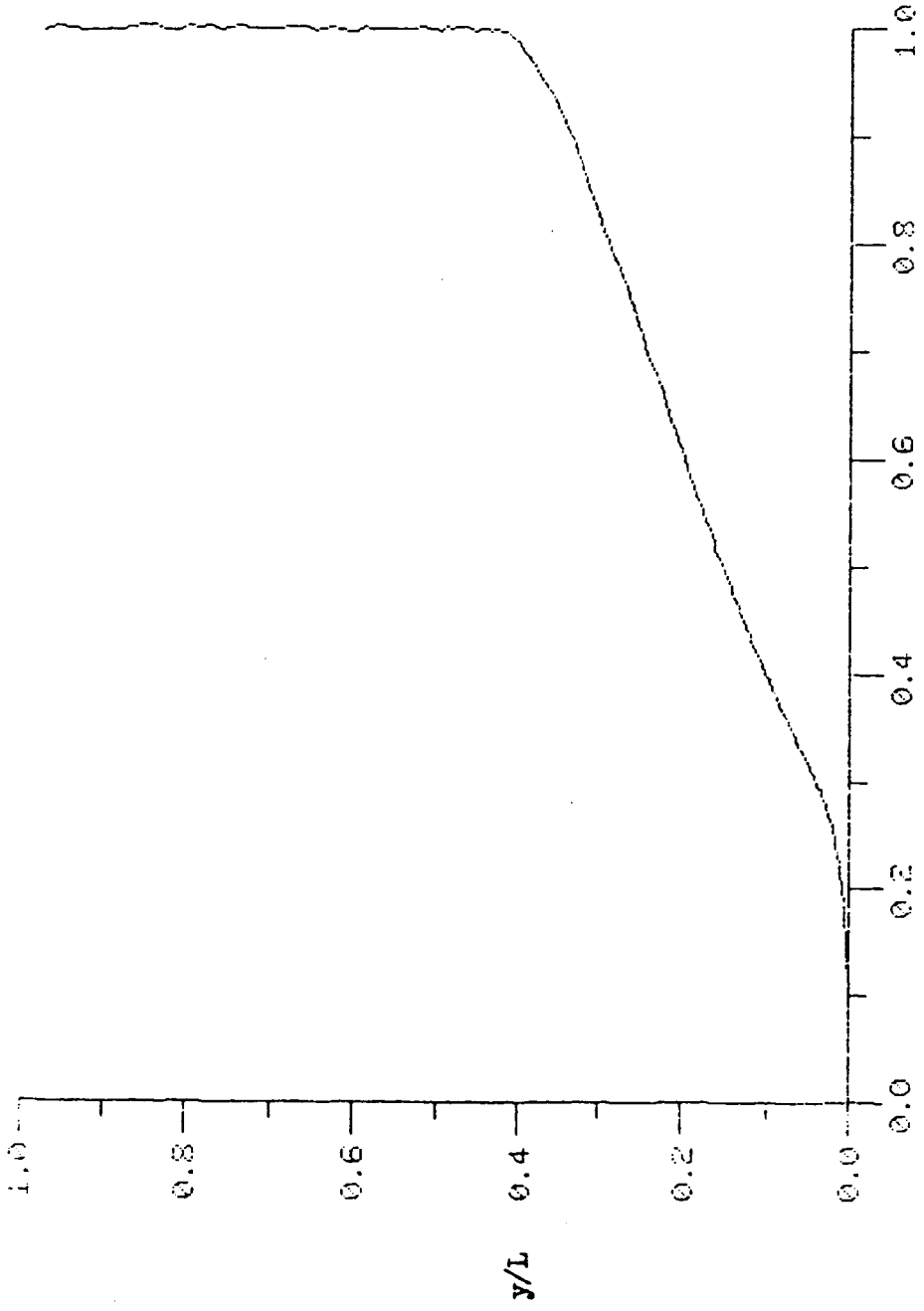

Figure 13c. Stagnation Temperature Profile at x=12.01

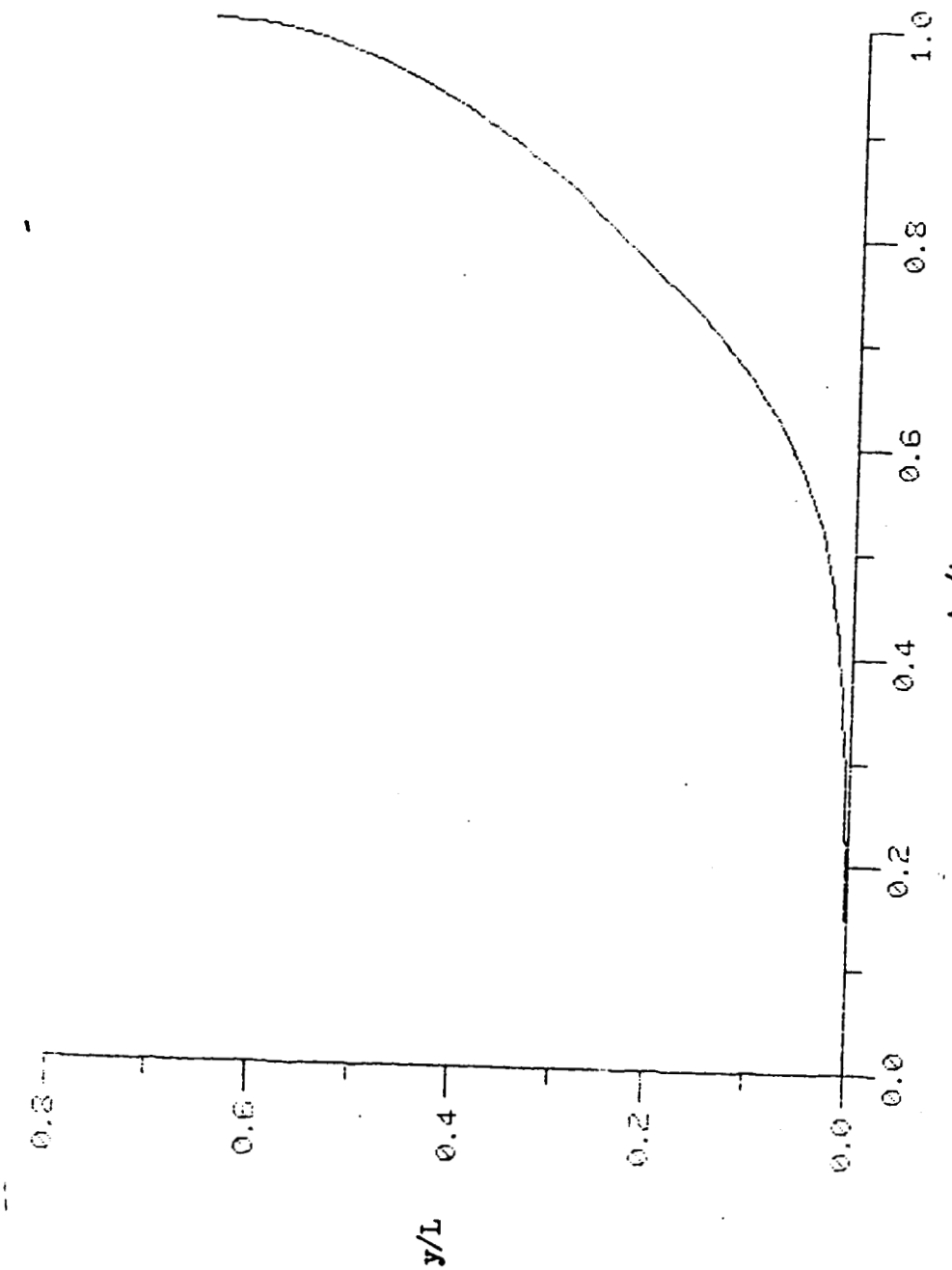

Figure 13d. Stagnation Temperature Profile at x=40.03

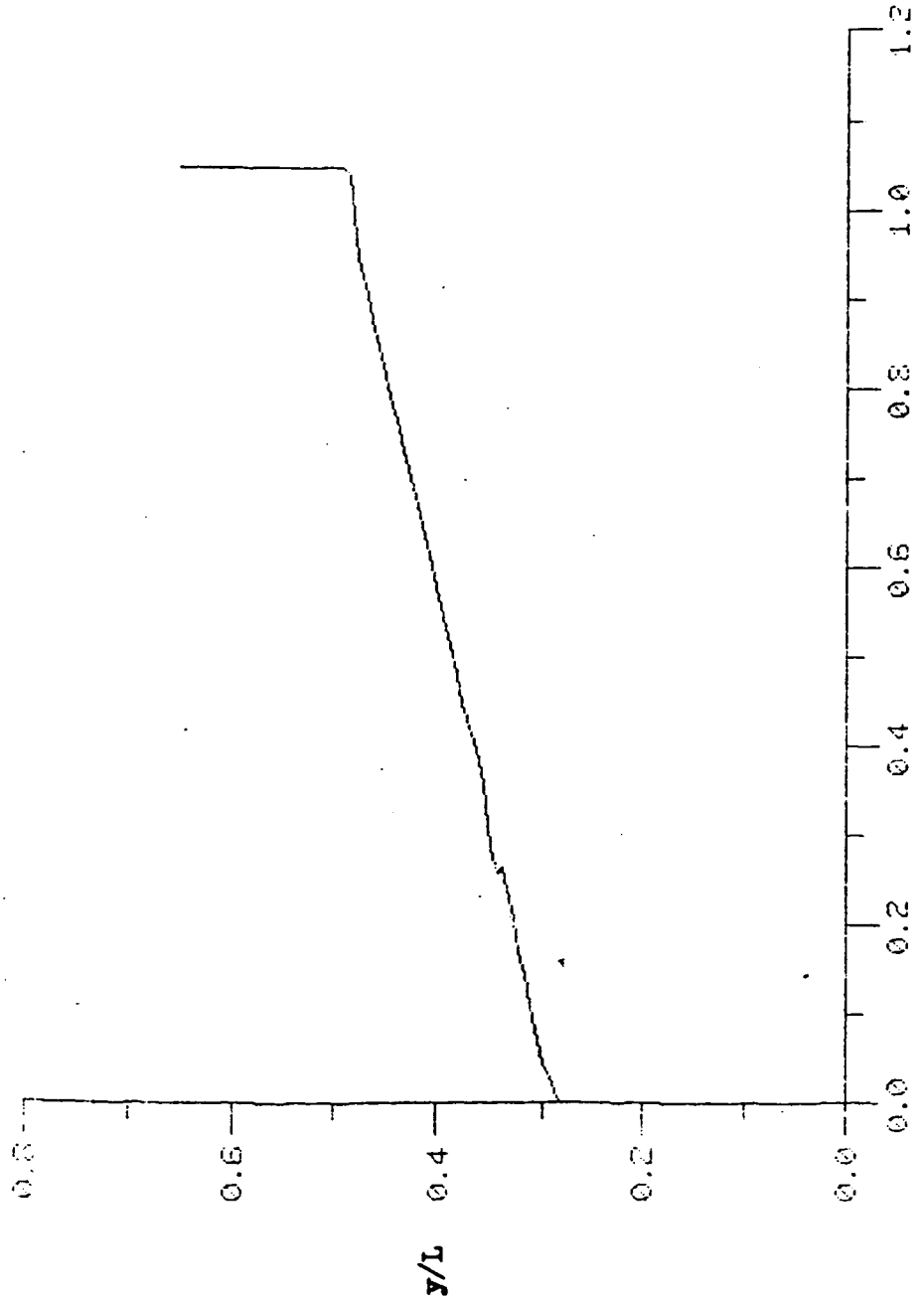

Figure 14a. Stagnation Pressure Profile at x=7.73

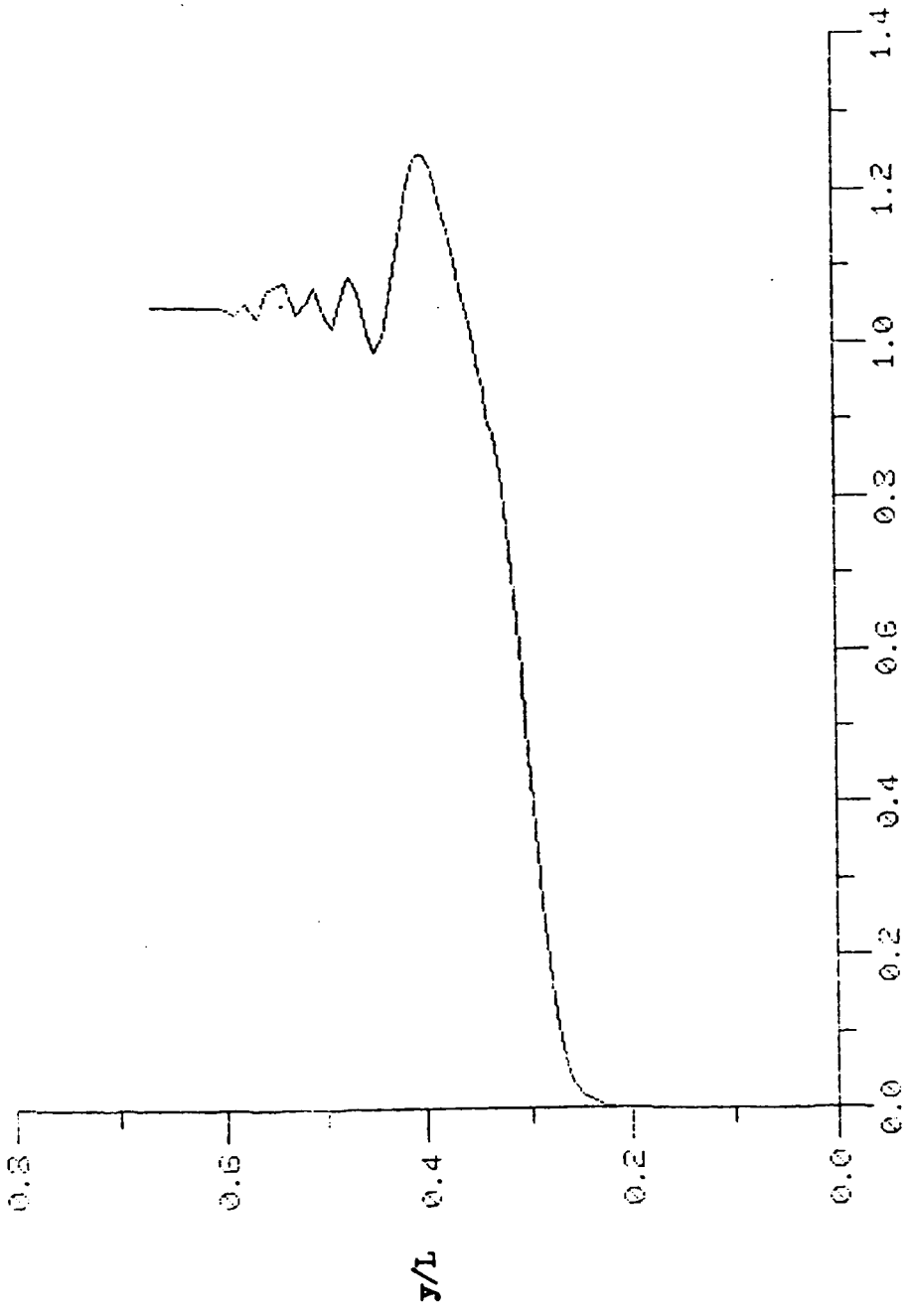

Figure 14b. Stagnation Pressure Profile at x=8.0

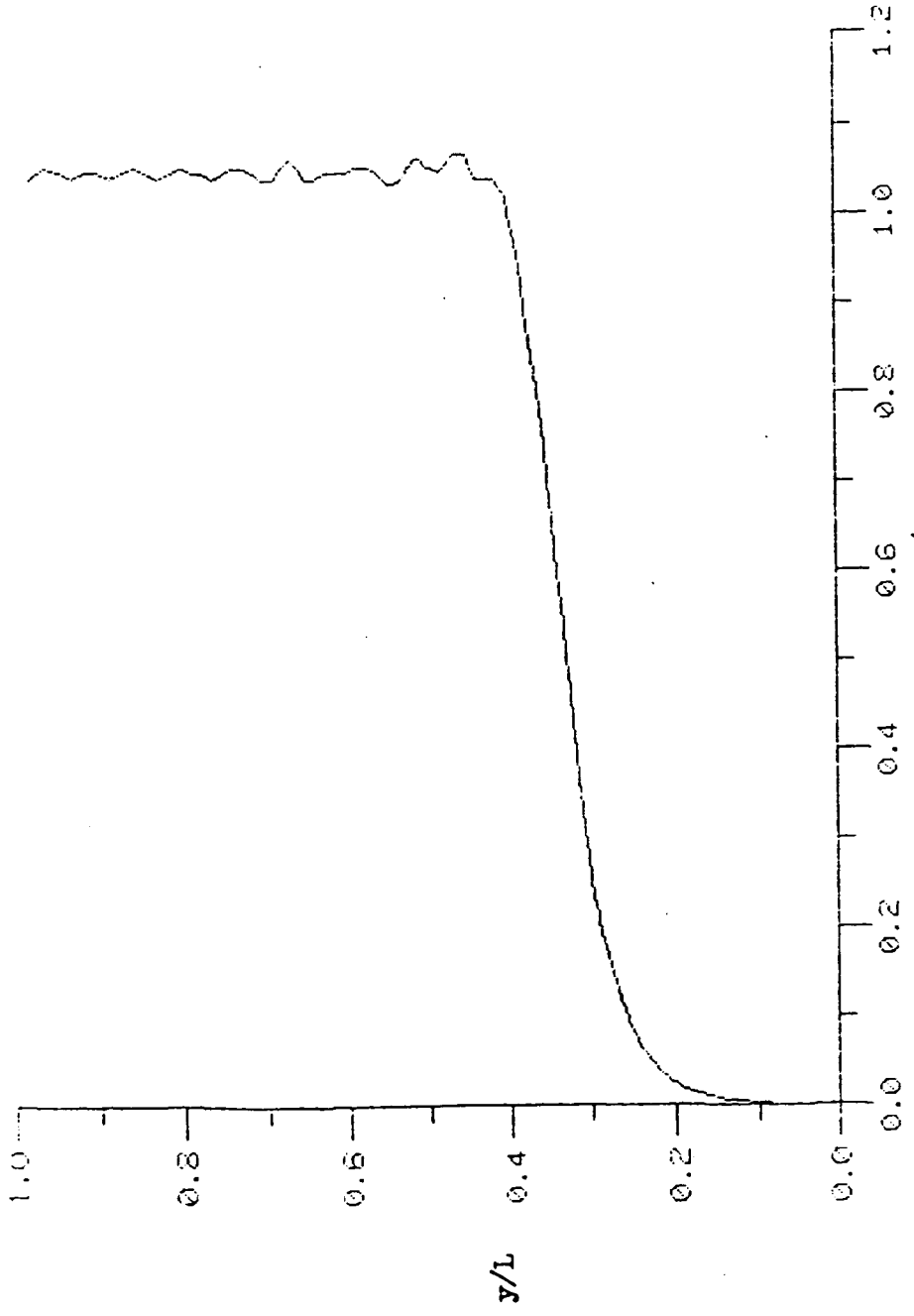

Figure 14c. Stagnation Pressure Profile at x=12.01

The stagnation pressure continued to increase showing the effect of the higher Mach number near the wall. Very near the wall, the velocity ratio was not determined from the 1/7th power law and thus the stagnation pressure profile was not linear. The profile, however, became linear at a small distance from the surface when boundary layer flow was encountered as can be seen in figure 14d.

F. Heat Transfer Rate Profiles

The heat transfer rate, $\dot{q}$, to the wall of the model was normalized by using the stagnation-point heating rate, $\dot{q}_s$, obtained by the method of Fay and Riddel [36]. At the distance beginning at the slot exit, the heat transferred to the surface of the model was small indicating that the nitrogen from the slot absorbed the heat that would have been felt on the surface of the model. As the mixing region developed, the heat transferred to the surface of the cone increased. Approaching the fully mixed region, the boundary layer thickness was increased and the heating rate to the surface was reduced.

The heat transfer profiles for slot to free-stream velocity ratios of 0.2, 0.5, 0.75 and 1.0 were plotted in figure 15. In the near slot region, increasing the slot to free-stream velocity ratio caused the heat transferred to the surface of the cone to increase. Since this increase in heating rate was mainly in the near slot region, the rate at which the fluid was ejected from the slot had a tremendous impact on the heat transfer rate in this region.

In general, the heat transferred to the surface in the mixing region decreased as the slot to free-stream velocity increased.

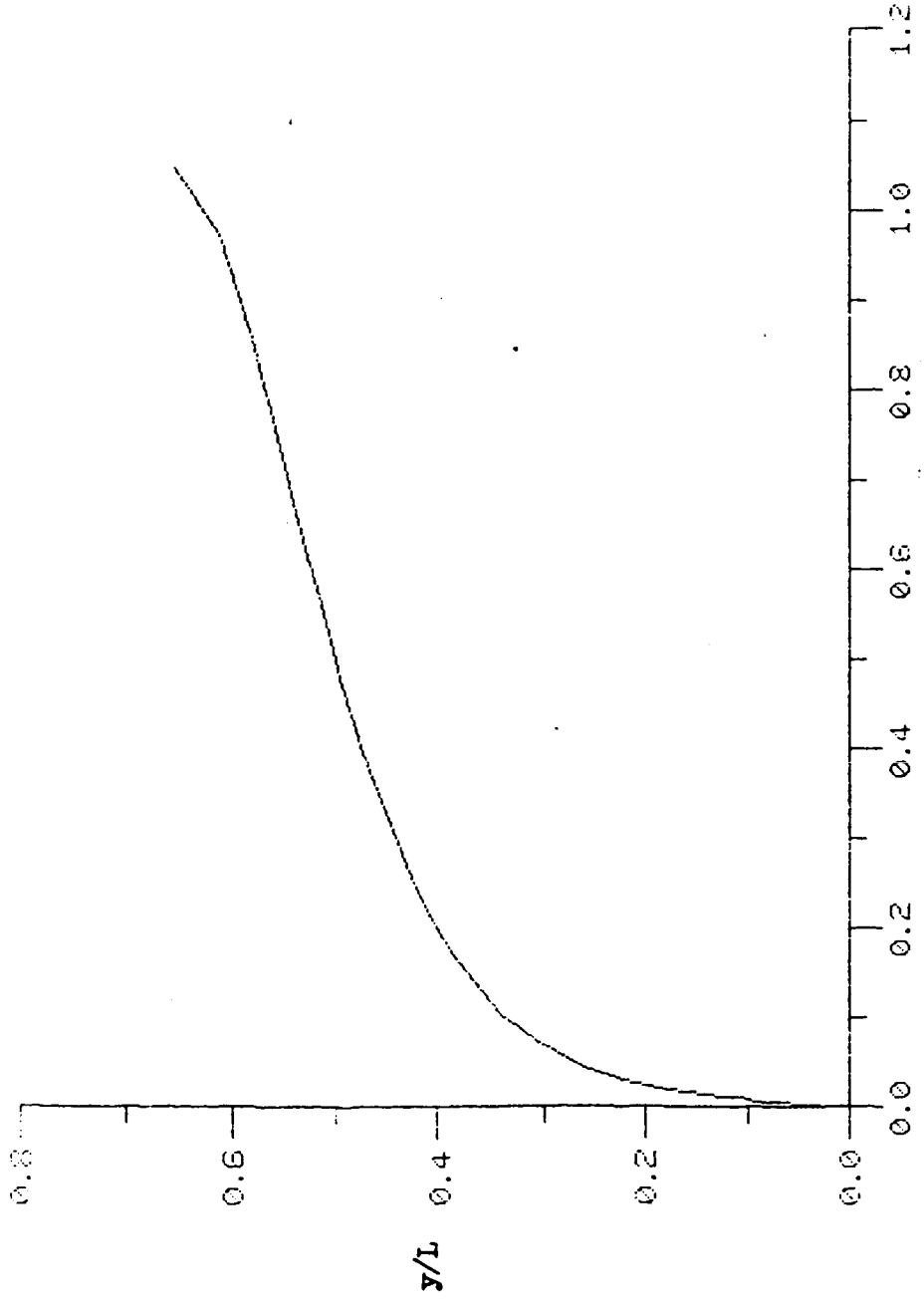

Figure 14d. Stagnation Pressure Profile at x=40.03

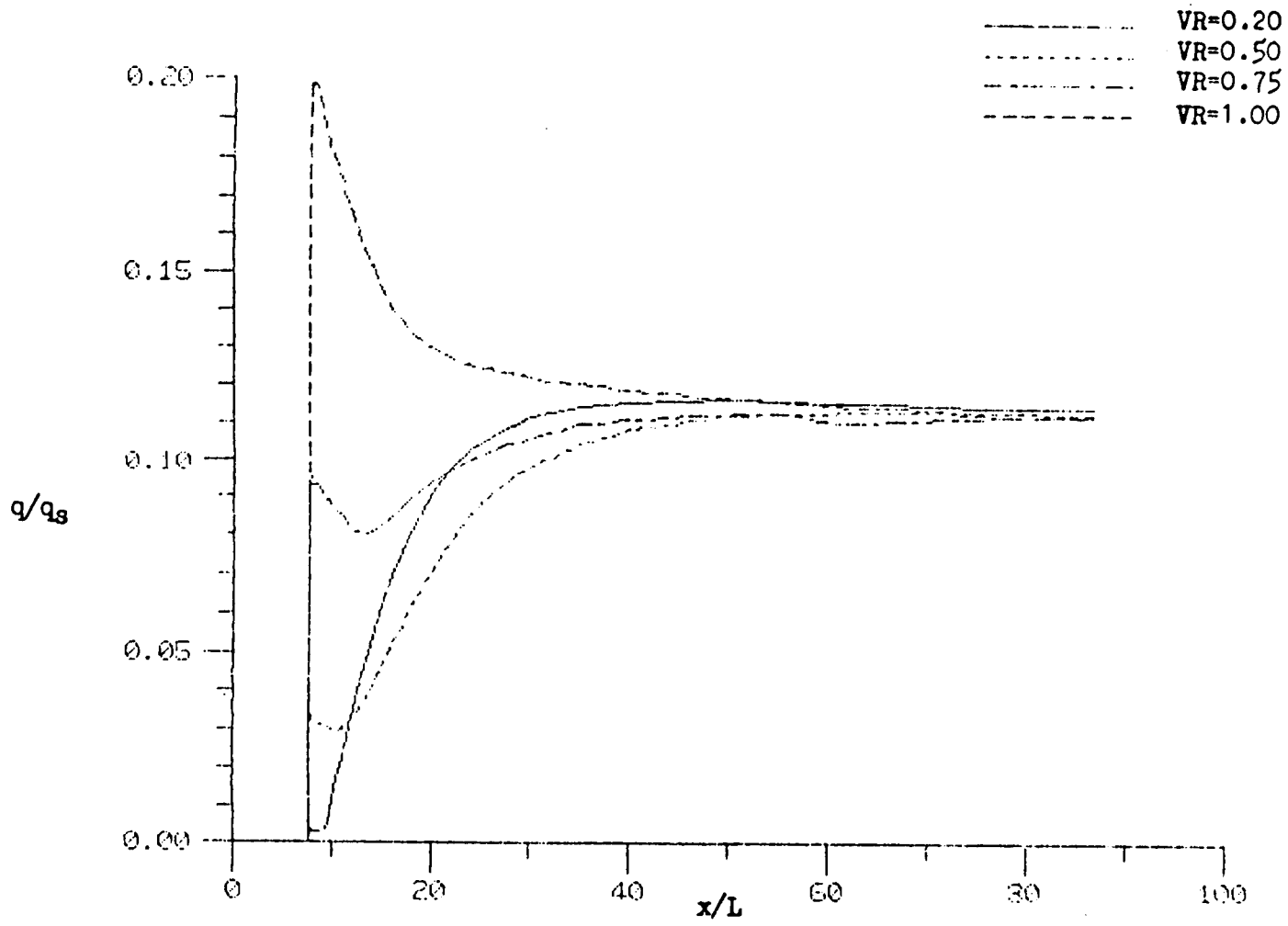

Figure 15. Heating Rates Distribution for Various Velocity Ratios

This decrease was very small and the downstream results actually showed the heating rates to be independent of velocity ratios. Increasing the slot to free-stream velocity ratio was more effective in decreasing the heat transferred to the surface of the cone downstream rather than immediately at the slot's exit.

To access the accuracy of the numerical method by Bushnell and Hefner [2], the numerical heating rates obtained from the computer program have been compared with heat transfer rates from a theoretical laminar study by Hamilton [4], and a theoretical turbulent study by Johnson and Rubesin [1]. The numerical results were also compared to the experimental correlations by Parthasarathy and Zakkay [5] as well as the experimental correlations of Zakkay et. al., [6].

The theoretical laminar heating rates under-predicted the numerical results while the theoretical turbulent heating rates over-predicted the numerical results. The numerical heating rates were also compared to known correlations from experimental studies. The correlations were valid only for downstream distances. The correlations from the experimental studies over-predicted the numerical heat transfer rates but compared better with the numerical results than the theoretical laminar and turbulent heat transfer rates as shown in figure 16. Since Zakkay's et. al., correlations compared more favorably to the numerical results than those of Parthasarathy and Zakkay, it was decided that further comparisons would only include the correlations of Zakkay et. al., [6]. Figures 17, 18 and 19 give numerical heating rates for velocity ratios of 0.5, 0.75, and 1.0 respectively. These

results were compared to the theoretical laminar and turbulent heating rates as well as the experimental correlations given by Zakkay et. al., [6]. Zakkay's et. al., results compared favorably in the downstream region at higher velocity ratios.

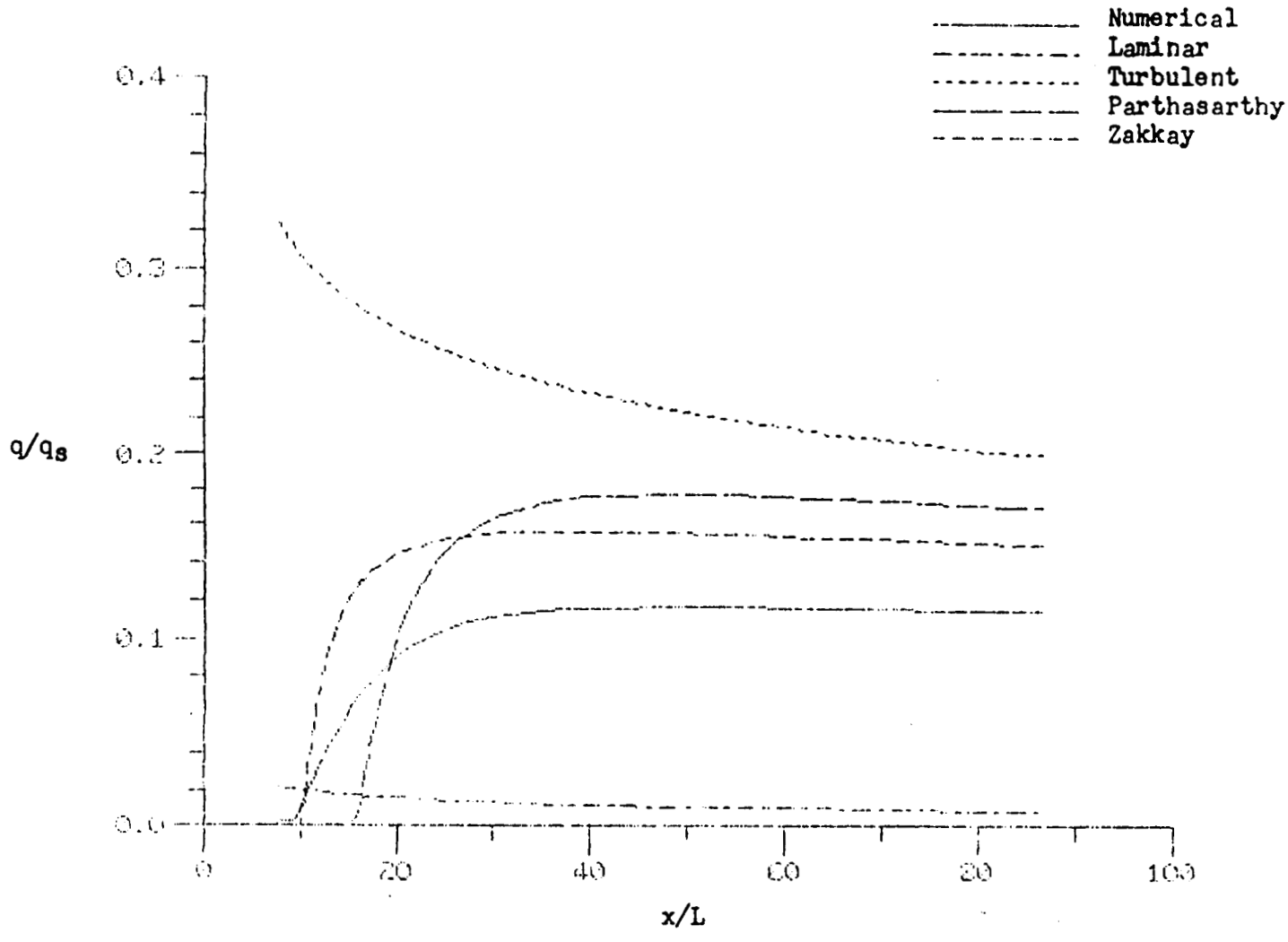

Figure 16. Heating Rates Distribution for Velocity Ratio = 0.2

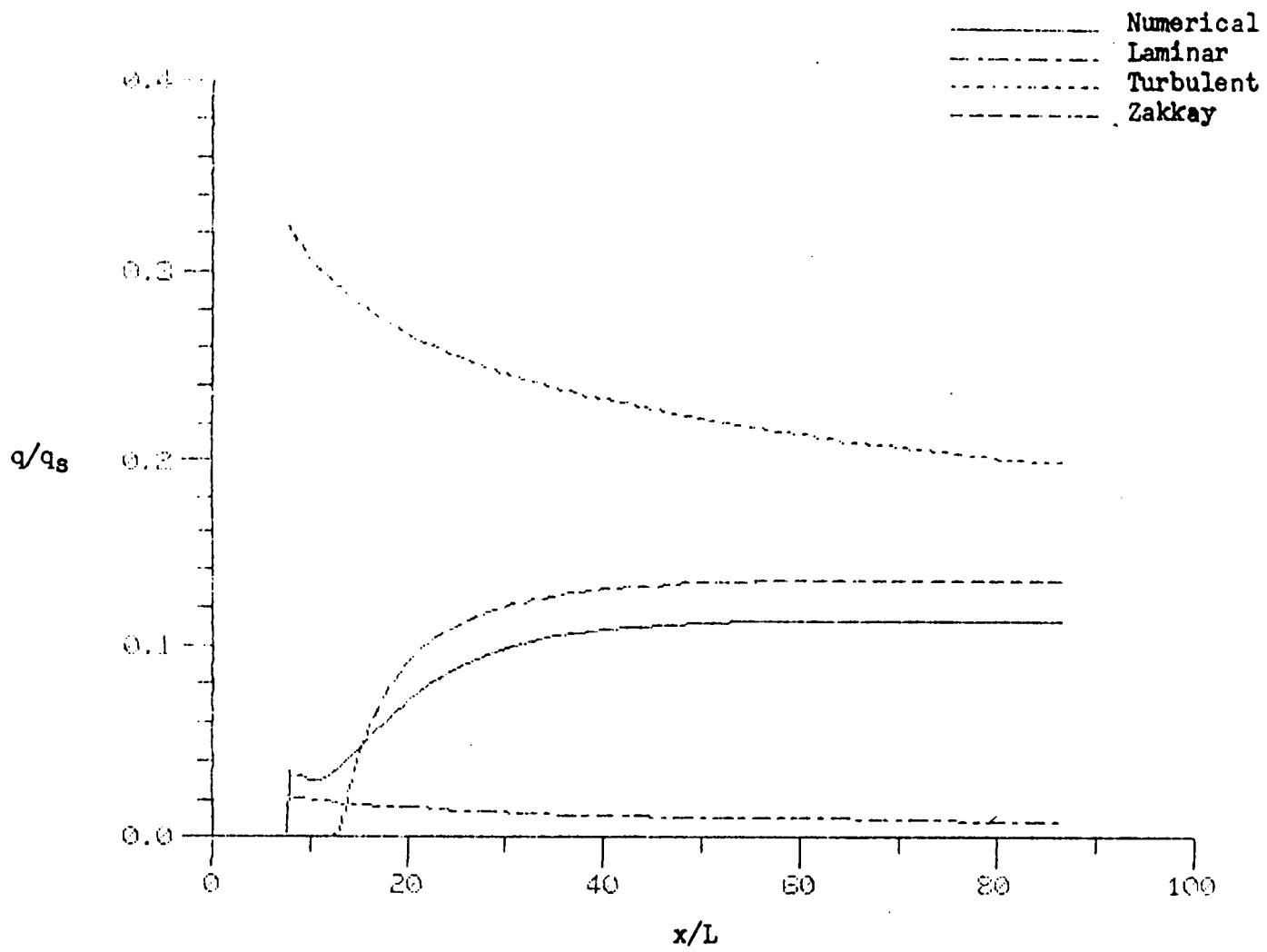

Figure 17. Heating Rates Distribution for Velocity Ratio = 0.5

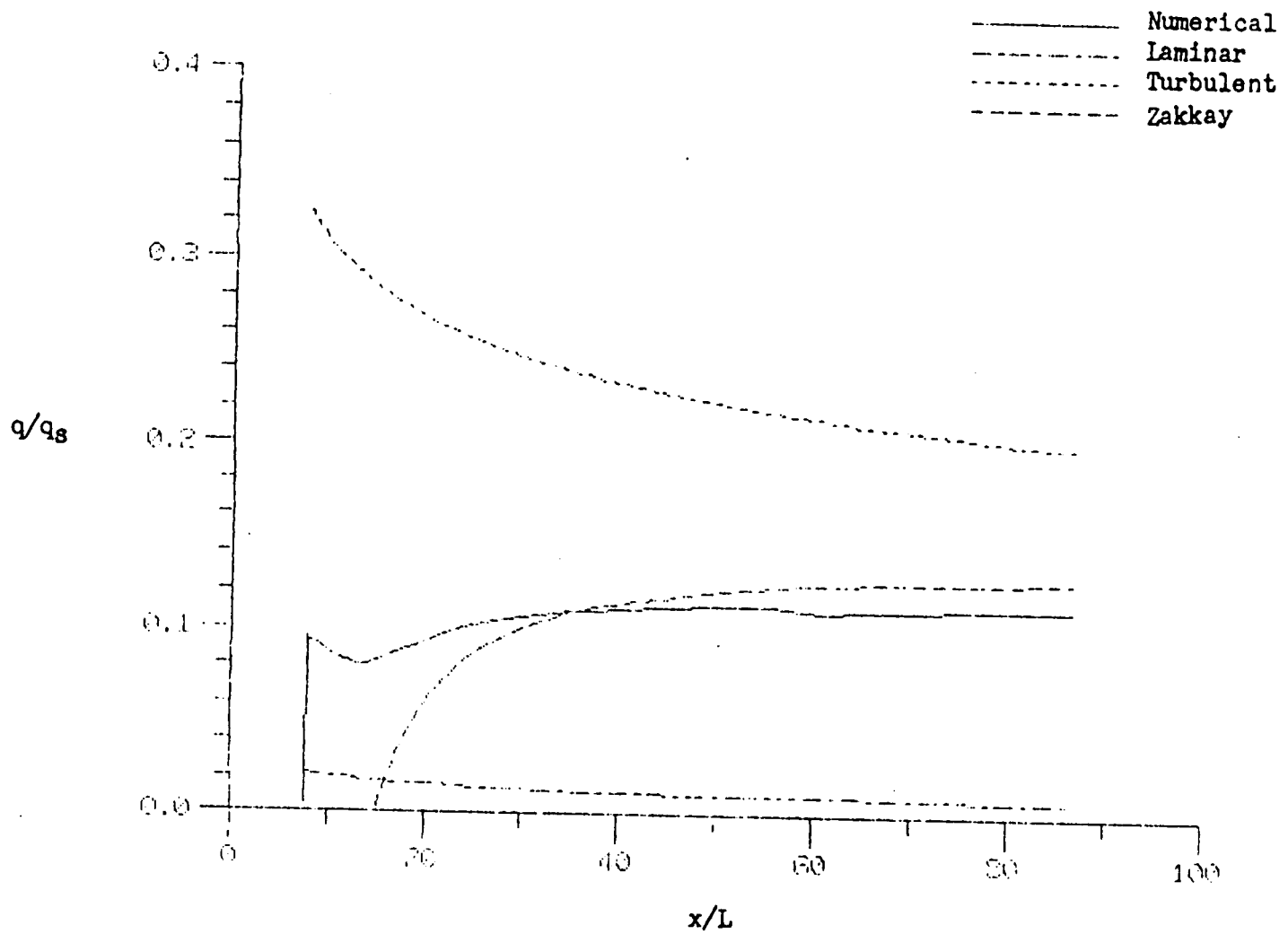

Figure 18. Heating Rates Distribution for Velocity Ratio = 0.75

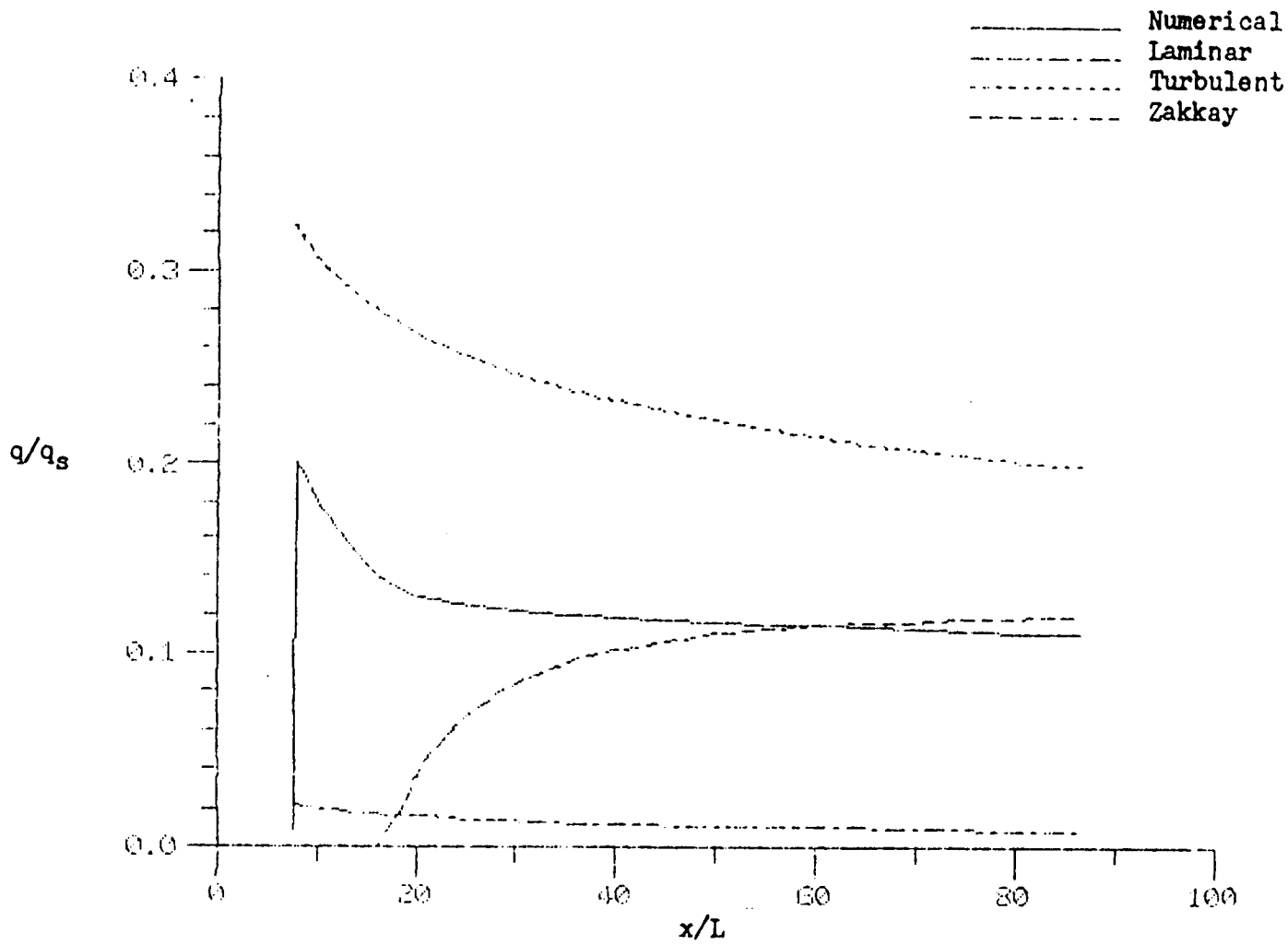

Figure 19. Heating Rates Distribution for Velocity Ratio = 1.0

CHAPTER VI

CONCLUSIONS AND RECOMMENDATIONS

A numerical method which solved the partial-differential equations for the mean motion of an axisymmetric compressible turbulent boundary layer with tangential injection by an implicit finite-difference procedure has been utilized to determine the heat transferred to the surface of a cone-shaped model for slot to free-stream velocity ratios of 0.2, 0.5, 0.75 and 1.0. The cone had a Mach number of 6.95 and a free-stream unit Reynold's number of 1.18×10^6 per foot. The velocity, temperature, Mach number stagnation temperature, and stagnation pressure profiles were also determined. Based on the numerical results, the following conclusions have been reached.

1. The numerical method clearly defines three distinct regions; the near slot region, the mixing region, and the fully mixed region.
2. In the slot lip region, the transition from constant, slot properties to constant free-stream properties is not well defined initially.
3. Near the slot's exit, increasing the slot to free-stream velocity ratio substantially increased the amount of heat transferred to the surface of the cone.

4. In the mixing region, an increase in the slot to free-stream velocity ratio decreased the heat transferred to the surface of the cone.
5. The theoretical turbulent heating rates by Johnson and Rubesin over-predicted the numerical heat transfer rates and the theoretical laminar heating rates by Hamilton under-predicted the numerical heat transfer rates.
6. The correlations from an experimental study by Zakkay, et. al., over-predicted the numerical heating rates but compared better than the theoretical turbulent and laminar heating rates.

These conculsions support the following recommendations for improving the accuracy of the present numerical method in predicting the heat transferred to the surface of a cone-shaped model.

1. The lip area should be investigated to determine what properties should be used during the transition from the constant slot properties to constant free-stream properties.
2. The size of the slot height should be investigated to determine the overall effects on the heating rates.
3. Since the matched pressure condition is an ideal case, an unmatched pressure conditon should be incorporated into the program to determine the effect of pressure gradients on the heating rates.

APPENDIX A

PRELIMINARY DATA

Nose: 3 inch cone-shaped with 0.243 inch tangential slots.

Angle of attach (α) = 0

Free-stream temperature (t_e) = 446 R

Free-stream Mach number (M_e) = 6.95

Free-stream specific heat ratio (γ) = 1.382

Free-stream specific heat at constant Pressure (C_p) = 0.260 Btu/(lbm · R)

Gas constant (R) = 55 (ft · lbf)/(lbm · R)

Prandtl number (Npr) = 0.743

Free-stream viscosity (μ_e) = 0.962E - 5 lbm/(ft · sec)

Free-stream thermal conductivity (k_e) = 0.321 btu/(ft · sec · R)

Stagnation heat transfer from Fay and Riddel ($\dot{q}_s$) = 86.8 btu/(ft^2 · sec)

Free-stream density (ρ_e) = 1.566E-3 lbm/ft^3

Free-stream velocity (u_e) = 7249 ft/sec.

Free-stream unit reynolds number (R_e) = 1.18E6/ft

Injected fluid: Nitrogen

Coolant exit temperature at slot = 577 R

Distance from centerline to edge of slot (S) = 7.732 inches

APPENDIX B

INPUT DATA FOR VELOCITY RATIO = 0.2
(ADAPTED FROM REFERENCE 35)

```
$NAM1
      NUMETA=300,
      NMAXF=240,
      NMAXG=220,
      DELETA=0.00015,
      XK=1.02,
      XI0=2.48627E5,
      DELXI0=0.3786E0,
      XITEST=.8E6,
      XISTOP=.37132139581092E8,
      FTAB=0.0,.0301,.0602,.0903,.1204,.1295,.1383,.1449,.1513,.1577,
      .1628,.1672,.1741,.1798,.1845,.1923,.1985,.1923,.1845,.1798,.1741,
      .1672,.1628,.1577,.1513,.1449,.1383,.125,.117,.108,.088,.079,.061,
      .045,.036,.020,.010,.005,.1,.2,.3,.4715,.5206,.5747,.6226,
      .7067,.7550,.7897,.8172,.8400,.8560,.8769,.8923,.9063,.9191,
      .9309,.9419,.9522,.9618,.9707,.9795,.9876,.9954,.99999,1.0,
      VWTAB=33*0.0,
      EPSLONE=0.05,
      EPSLONW=0.01,
      UEDSTAB=33*0.9489,
      GTAB=38*1.E-20,27*1.0,
      WEDS2HE=0.,
      PR=.743,
      ZETWTAB=33*.1228,
      XNBAR=0.8,
      RERSTAB=33*.1659,
      CAPRS=1.149E5,
      RTAB=3.4411,3.773,4.1049,4.4368,4.7688,5.1007,5.4326,
           5.7645,6.0964,6.7728,7.4492,8.1255,8.8019,9.4783,
           10.1547,10.8310,11.5074,11.9132,12.3191,12.7249,
           13.1307,13.5365,13.9424,14.3482,14.754,15.4304,
           16.1068,16.7831,17.4595,18.1359,18.8123,19.4886,
           20.165,
      J=1,
      SHE=0.04248,
      HSHE=1.,
      ZETATAB=.1228,.1236,.1261,.1302,.1359,.1379,.1401,.1417,.1435,
      .1452,.1467,.1480,.1501,.1520,.1535,.1562,.1583,.1562,.1535,.1520,
      .1501,.1480,.1467,.1452,.1435,.1417,.1401,.1369,.1352,.1328,
      .1273,.1236,.1191,.1152,.1121,.1090,.1063,.1039,.1117,.1374,
      .1811,.2997,
      .3436,.3970,.4486,.5493,.6128,.6611,.7009,.7394,.7593,.7920,.8165,
      .8392,.8602,.8799,.8984,.9160,.9325,.9480,.9635,.9778,.9917,.9986,.9999,
      XL=7.732,9.2655,10.7990,12.3325,13.866,15.3995,16.933,
         18.4665,20.,23.125,26.25,29.375,32.5,35.625,38.75,
         41.875,45.,46.875,48.75,50.625,52.5,54.375,56.25,
         58.125,60.,63.125,66.25,69.375,72.5,75.625,78.75,81.875,
         85.,
      NUMX=33,
      NUMY=65,
      YL=0.0,.0009,.0018,.0027,.0036,.0061,.0097,.0134,.0182,.0243,.0304,
      .0365,.0486,.0608,.0729,.0972,.1215,.1458,.1701,.1823,.1944,.2066,
      .2126,.2187,.2248,.2296,.2333,.236,.240,.244,.248,.252,.256,
       .260,.264,.268,.272,.276,.278,.280,.282,.284,.285,
      .287,.290,.30,.31,.32,.33,.34,.35,.36,.37,.38,
      .39,.40,.41,.42,.43,.44,.45,.460,.470,.475,200.,
      X0=7.732,
      OL=.0834,
      DUDXTAB=33*0.0,
      DZDXTAB=33*0.0,
```

```
      FR0=0.89,
      AP=0.265,
      BP=-0.196,
      CP=.0438,
      ABTAB=60.,26.,18.5,14.8,12.5,11.2,10.,9.1,6.,3.8,3.0,
      FCFTAB=-1.,0.,1.,2.,3.,4.,5.,6.,12.,24.,100.,
      NFCFAB=11,
      PRTTAB=4*.9,
      YDDPRT=0.,0.5,1.0,15.,
      NYP=4,
       XLPR=7.732,7.8,7.9,8.0,8.5,9.0,9.5,10.,10.5,11.,12.,13.,14.,15.,
            16.,18.,20.,22.,24.,26.,28.,30.,35.,37.32,40.,50.,
            55.,60.61,65.,70.,75.,80.57,85.,
      IVEG=3,
      INIT=0,
      IUSEEMU=1,
      MPWEMU=1,
      YCDL=.1215,
      TDL=0.0400,
      YDEL0=0.758,
      SNT=.8,
      SM=.7,
      A2=.09,
      A1=.14,
      IFBLU=0,
      IWLDMP=0,
       AKDUM=1.8,
$
```

REFERENCES CITED

1. Johnson, H. A. and Rubesin, M. W., "Aerodynamic Heating and Convective Heat Transfer-Summary of Literature Survey," Trans. ASME, Vol. 71, No. 5, July 1949, pp. 447-456.

2. Beckwith, I.E. and Bushnell, D. M., "Calculation by a Finite Difference Method of Supersonic Turbulent Boundary Layers with Tangential Slot Injection," NASA TND-6221, April 1971.

3. Nowak, R. J., Albertson, C. W., and Hunt, L. R., "Aerothermal Tests of a 12.5 Cone at Mach 6.7 for various Reynolds numbers, Angles of Attach, and Nose Shapes," NASA TP-2345.

4. Hamilton, H. Harris,II: "Calculation of Laminar Heating Rates on Three-Dimensional Configurations using the Axisymmetric Analogue," NASA TP-1698, 1980.

5. Parthasarthy, K. and Zakkay, V., "An Investigation of Turbulent Slot Injection at Mach 6," AIAA Journal, Vol. 8, July 1970.

6. Zakkay, V., Wang, Chi R., and Miyazawa, M., "Effect of Adverse Pressure Gradient on Film Cooling Effectiveness," AIAA paper, No. 73-697, July 1973.

7. Beckwith, I.E., "Recent Advances in Research on Compressible Turbulent Boundary Layers," NASA, Langley Research Center, 1970.

8. Goldstein, R. J., "Film Cooling", Advances in Heat Transfer, Vol. 7, Academic Press, New York, 1971.

9. Hefner, J. N., "Effect of Geometry Modifications to Effectiveness of Slot Injection in Hypersonic Flow," AIAA Journal, Vol. 14, No. 6, June, 1976.

10. Ko, S. Y. and Liu, K. Y., "Experimental Investigations on Effectiveness, Heat Transfer Coefficient and Turbulence of Film Cooling," AIAA Journal, Vol. 18, No. 8, August 1980.

11. Zakkay, V and Wang, C. R., "Investigation of Multiple Slot Film Cooling to a Blunt Nose Cone," AIAA paper, No. 73-698 July, 1973.

12. Zakkay, V., Sakell, L. and Parthasarthy, K., "An Experimental Investigation of Supersonic Slot Cooling," Paper presented at the 1970 Heat Transfer and Fluid Mechanics Institute, June 10 - 12, 1970. Published by Stanford University Press.

13. Larue, J. C. and Libby, P. A., "Further Results Related to the Turbulent Boundary Layers with Slot Injection of Helium," Physics of Fluids, Vol. 23, No. 6, June, 1980.

14. Mironov, V. N., Vasechkin, V. M., Manonov and Yarygina, N. I., "Heat and Mass Transfer at High Free-Stream Turbulence as a Function of Injection Rate," Heat Transfer Soviet Research, Vol. 13, No. 5, September - October,.1981.

15. Yu, Vasil'ev and Petrov, M.D., "Influence of Tangential Injection on Heat Transfer to a Cone in the Transition Reynolds Number Domain," Fluid Dynamics, September - October, 1977. pp. 662-666.

16. Foster, R. C. and Haji Skeikh, A., "An Experimental Investigation of Boundary Layer and Heat Transfer in the Region of Separated Flow Downstream of Normal Injection Slots," Journal of Heat Transfer, No. 2, May, 1975.

17. Best, R., "Investigation on the Cooling Effectiveness of Tangentially and Normally Injected Coolant Flows," German Chemical Engineering, Vol. 2, pp. 343-351, 1979.

18. Cary, A. M. and Hefner, J. N., "Film Cooling Effectiveness and Skin Friction in Hypersonic Turbulent Flow," AIAA Journal, Vol. 10, No. 9, September, 1972.

19. Richards, B. E., and Stollery, J. L., "Laminar Film Cooling Experiments in Hypersonic Flow," J. Aircraft, Vol. 16, No. 3, March, 1979.

20. Eiswirth, E. A., Kupp, H. W., Brandon, H. J. and Masek, R. V., "An Experimental Investigation of Ogive Film Cooling," ASME paper 76-ENAS-39, July, 1976.

21. Hefner, J. N. and Cary, A. M., "Swept Slot Film Cooling Effectiveness in Hypersonic Turbulent Flow," J. Spacecraft, Vol. 11, No. 5, May, 1974.

22. Hefner, J. N., Cary, A. M., and Bushnell, D. M., "Investigation of the Three-Dimensional Turbulent Flow Downstream of Swept Slot Injection in Hypersonic Flow," AIAA paper, No. 74-679 and ASME paper No. 74-HT-13.

23. Rastogi, A. K., and Whitelaw, J. H., "The Effectiveness of Three-Dimensional Film Cooling Slots-I. Measurements," International Journal of Heat and Mass Transfer, Vol. 16, 1665 - 1672, 1973.

24. Larue, J. C. and Libby, P. A., "Measurements in Turbulent Boundary Layer with Slot Injection of Helium," Physics of Fluids, Vol. 20, No. 2., February, 1977.

25. Saad, M. A., and Miller, J. A., "Proceedings of the 1966 Heat Transfer and Fluid Mechanics Institute," June 22 - 24, 1966 Published by Stanford University Press, 1966.

26. Plostins, P. and Rubin, S. G., "The Axisymmetric Stagnation Region Full Shock Layer for Large Rates of Injection," Numerical Heat Transfer, Vol. 4, pp. 359 - 375, 1981.

27. Patankar, S. V., and Spalding, D. B., "A Finite-Difference Procedure for Solving the Equations of the Two-Dimensional Boundary Layer," International Journal of Heat and Mass Transfer, Vol. 10, 1967, pp. 1389 - 1411.

28. Metzger, D. E., Carper, H. J. and Warren J. M., "Predicted Film Cooling Near Flush Slots-Comparison with Experiment," AIAA paper No. 72-291, April 1972.

29. Starkenberg, J., and Creci, R. J., "Boundary-Layer Transition on a Film-Cooled Slender Cone," AIAA J., Vol. 14, April, 1976.

30. Lin, T. C., and Rubin, S. G., "Viscous Flow Over a Cone. Part 2. Supersonic Boundary Layer," Journal of Fluid Mechanics, Vol. 59, Part 3, July 1973, pp. 593 - 620.

31. Cary, A. M., Bushnell, D. M., and Hefner, J. N., "Predicted Effects of Tangential Slot Injection on Turbulent Boundary Layer Flow Over a Wide Speed Range," Journal of Heat Transfer, Vol. 101, No. 4, pp. 699 - 704, November, 1979.

32. Cary, A. M. and Hefner, J. N., "An Investigation of Film Cooling Effectiveness and Skin Friction in Hypersonic Turbulent Flow," AIAA paper No. 71-599, June, 1971.

33. White, Frank M., Viscous Fluid Flow, 1st ed. (New York: McGraw-Hill, 1974).

34. Miner, W. E., and Lewis, C. H., "A Finite-Difference Method for Predicting Supersonic Turbulent Boundary Layer Flows with Tangential Slot Injection," NASA CR-2124, October, 1972.

35. Hixion, B. A., Beckwith, I.E. and Bushnell, D. M., "Computer Program for Compressible Laminar of Turbulent Nonsimilar Boundary Layers," NASA TMX-2140, April 1971.

36. Fay, J. A. and Riddell, F. R., "Theory of Stagnation Point Heat Transfer in Dissociated Air," Journal of the Aeronautical Sciences, Vol. 25, No. 2, February, 1958, pp. 73 - 85.